

# Amino Acid-Containing Polyacetylenes: Synthesis, Hydrogen Bonding, Chirality Transcription, and Chain Helicity of Amphiphilic Poly(phenylacetylene)s Carrying L-Leucine Pendants

Kevin K. L. Cheuk, Jacky W. Y. Lam, Junwu Chen, Lo Ming Lai, and Ben Zhong Tang\*

Department of Chemistry, Institute of Nano Science and Technology, and Open Laboratory of Chirotechnology of the Institute of Molecular Technology for Drug Discovery and Synthesis,<sup>†</sup> Hong Kong University of Science and Technology, Clear Water Bay, Kowloon, Hong Kong, China

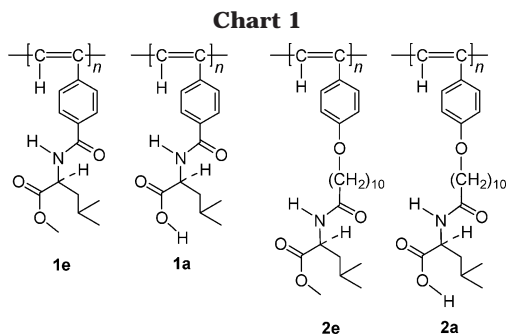
Received April 9, 2003; Revised Manuscript Received June 13, 2003

**ABSTRACT:** L-Leucine–phenylacetylene adducts **6** and **14** undergo self-association in concentrated solutions and heterocomplexation with solvent molecules through hydrogen bond formation. The adducts are polymerized by rhodium catalysts into poly(4-ethynylbenzoyl-L-leucine methyl ester) (**1e**) and poly-[11-(4-ethynylphenoxy)undecanoyl-L-leucine methyl ester] (**2e**), with the polymerizations of **6** producing polymers with high molecular weights ( $M_w$  up to  $1.47 \times 10^6$ ) and high stereoregularity (*Z* content up to 100%) in high yields (up to 92%). The ester groups of “polyesters” **1e** and **2e** are selectively hydrolyzed under basic conditions to afford “polyacids” **1a** and **2a** carrying free leucine pendants. The polymers are thermally stable (up to  $\sim 260$  °C) and undergo *Z–E* isomerization at  $\sim 200$  °C. The chirality transcription from the L-leucine pendants induces the chain segments of polymers **1** to helically spiral predominantly in one preferred direction, while the helicity induction processes in **2** are interrupted by the relaxations of the long flexible spacers between the chiral pendants and the polyene backbones. The chiroptical properties of the amphiphilic polymers change with solvent. In nonpolar solvents, **1** shows high optical activities and strong Cotton effects, whose helical structures are stabilized by intra- and interchain hydrogen bonding. The chain helicity of the polymers decreases in polar solvents due to the partial breakage of the hydrogen bonds within and between the polymer strands.

## Introduction

In the living world, nature utilizes covalent forces to knit small building blocks such as amino acids to make macromolecules such as proteins, which are further organized into higher-order supramolecular structures by noncovalent forces.<sup>1</sup> One structural motif frequently utilized by nature in the assembling processes is helix, which is expressed at all levels of organizational hierarchy: e.g.,  $\alpha$ -helix of proteins, double helix of DNA, triple helix of collagen, helical coat of tobacco mosaic virus, and spiral bacterium of *Spirillum*.<sup>2</sup> While various noncovalent forces are involved in the formation of the helical structures, hydrogen bonding is beyond doubt the most important driving and stabilizing force in the bioassembling processes.<sup>3</sup> Learning from nature, scientists have made synthetic polymers with helical conformations.<sup>4</sup> In many such polymer systems, it has been speculated that hydrogen bonding induces and maintains the helical structures.<sup>5–7</sup> Detailed studies on the hydrogen-bond formation and its effects on chain helicity in the synthetic polymer systems have, however, been rarely performed.

We are interested in creating helical macromolecules by hybridizing synthetic hydrophobic conjugated polymers with naturally occurring hydrophilic building blocks at the molecular level.<sup>8,9</sup> It is envisioned that the hybrid descendants may be both semiconductive and biocompatible. Such cytophilic molecular wires may find

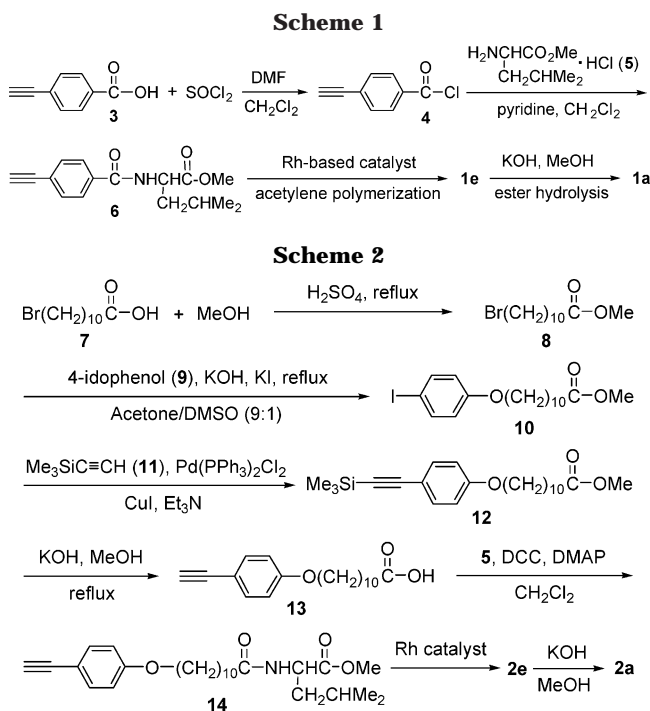


bioelectronic applications, e.g., as biosensors in medical diagnosis, as controllers in drug delivery, and, more exotically, as artificial nerves in cytotech nanorobotics.<sup>10</sup> The amphiphilic polymers may emulate the behaviors of biopolymers, thus offering a simple artificial model system for the studies of complex natural systems. In our previous work,<sup>11</sup> we attached pendants of L-valine (Val), an amino acid commonly found in proteins, to the backbone of poly(phenylacetylene) (PPA), the best-known photoconductive polyacetylene.<sup>12</sup> The Val–PPA hybrids formed helical structures and self-assembled into biomimetic morphologies, in which hydrogen bonding was believed to play a vital role.

In this work, we incorporated another common amino acid, L-leucine (Leu), into the PPA structure and synthesized a group of Leu-containing PPA derivatives (**1** and **2**; Chart 1). We examined whether the Leu pendants could also induce the PPA backbone to helically rotate and, if so, how the internal and external perturbations such as molecular structures and environmental variations would affect the chain helicity of the Leu–

<sup>†</sup> An Area of Excellence (AoE) Scheme administrated by the University Grants Committee of Hong Kong.

\* Corresponding author: phone +852-2358-7375; Fax +852-2358-1594; e-mail tangbenz@ust.hk.



PPA hybrids. Special efforts were made to elucidate the hydrogen-bond interactions in the polymer systems.

## Results and Discussion

### Monomer Preparation and Hydrogen Bonding.

We designed two leucine–phenylacetylene (Leu–PA) adducts, in one of which the Leu moiety is directly attached to the phenyl ring via a rigid amide bond (**6**; Scheme 1), while in another, the Leu moiety is separated from the phenyl ring by a flexible decyl spacer (**14**; Scheme 2). We vary the molecular structure in this way, in an effort to understand the chiral transcription processes in the polymer systems or, more specifically, to learn how the chirality of the Leu pendant is transcribed to the helicity of the PPA backbone, after the monomers have been polymerized. We are intrigued to know how the alkyl spacer will affect the chiral transcription or whether the Leu chirality in polymers **2** will induce the PPA chain to spiral, when the pendant and the backbone are separated far apart by 10 methylene groups.

The Leu–PA monomers (**6** and **14**) are prepared by respective amidations of 4-ethynylbenzoic acid (**3**)<sup>13</sup> and 11-[(4-ethynyl)phenoxy]undecanoic acid (**13**) with L-leucine methyl ester hydrochloride (**5**). Precursor **3** is first converted to its reactive acid chloride intermediate (**4**) by the reaction with  $\text{SOCl}_2$ ; nucleophilic substitution of the electrophile by **5** under a basic condition yields the desired monomer (**6**; Scheme 1). Acid **13** is prepared from **7** via multistep reactions (Scheme 2). In a dichloromethane (DCM) solution containing catalytic amounts of 1,3-dicyclohexylcarbodiimide (DCC) and 4-(dimethylamino)pyridine (DMAP), **13** is transformed by the reaction with **5** to its amide derivative, giving a white solid of monomer **14**. All the reactions proceed smoothly, and the products are isolated in high yields. The purified products all give satisfactory spectroscopic analysis data (see Experimental Section for details).

It is well-known that amino acids and peptides in biological systems form hydrogen bonds.<sup>14</sup> Will the Leu moiety in the Leu–PA adducts also form hydrogen

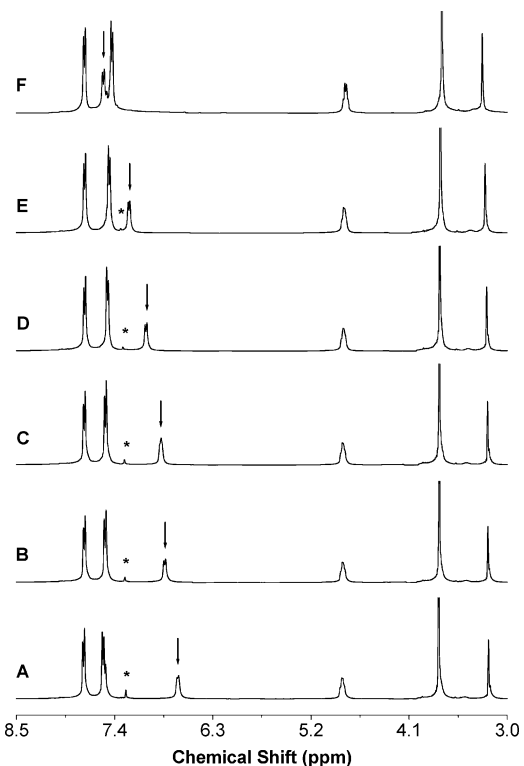


**Figure 1.**  $^1\text{H}$  NMR spectra of chloroform- $d$  solutions of **6** with varying concentrations (mg/mL): (A) 50, (B) 78, (C) 100, (D) 150, (E) 200, and (F) 300. The resonance peaks of the amide proton (HNCO) are marked with downward arrows ( $\downarrow$ ), while those of the solvent are marked with asterisks (\*).

bonds? To answer this question, we studied their NMR spectra. NMR spectrometry is a powerful tool for experimentally investigating hydrogen-bonding processes.<sup>15,16</sup> When a proton is involved in hydrogen bonding, its electrons are shared by two electronegative elements and its electron density is hence decreased. As a result, it is deshielded and comes into resonance at a lower field.<sup>16</sup> For intermolecular hydrogen bonding, its extent is affected by environmental conditions (solvent, concentration, etc.). In a nonpolar solvent, the degree of hydrogen bonding increases with an increase in the solution concentration, leading to a downfield shift in the resonance peak of the proton.<sup>16</sup>

We measured the NMR spectra of the Leu–PA adducts under different conditions. Figure 1 shows the  $^1\text{H}$  NMR spectra of deuteriochloroform solutions of **6** with different concentrations at room temperature. The weighted average position of the resonance peak of its amide proton changes with the variation in the concentration in the aprotic solvent. The dilute solution of **6** (50 mg/mL) exhibits a resonance peak of amide proton at  $\delta \sim 6.7$  (marked with a downward arrow in Figure 1A). When the concentration is increased to 78 mg/mL, a similar spectrum is observed, but the amide resonance is moved to  $\delta \sim 6.8$ . Further gradual increase in concentration progressively downfield shifts the amide resonance. When the solution concentration is increased to 300 mg/mL, the amide resonance is shifted to as far as  $\delta \sim 7.6$  (Figure 1F). Clearly, the amide protons are deshielded due to the formation of intermolecular hydrogen bonds accompanying the solution thickening.

Plotting the NMR data reveals that the peak position of the amide resonance downfield shifts with an increase in the concentration of the chloroform solution in a linear fashion (Figure 2). This suggests that the population

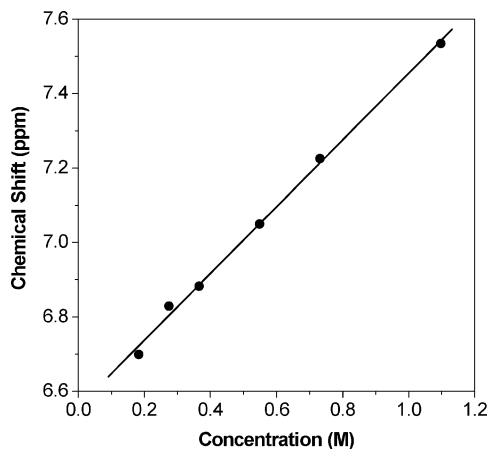
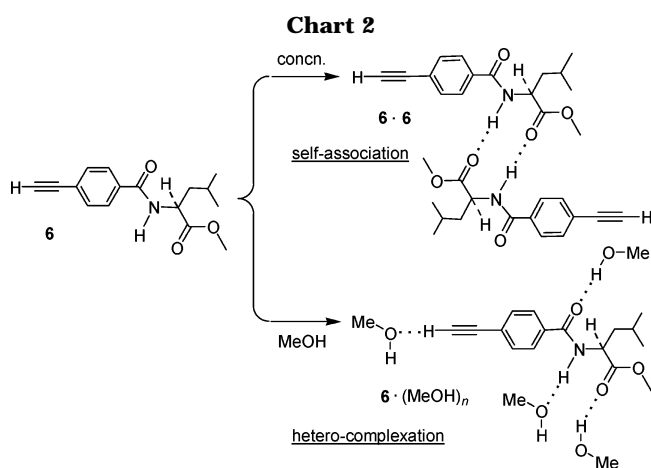


**Figure 2.** Concentration dependence of the chemical shift of the resonance peaks of the amide proton of the chloroform-*d* solutions of **6**.



of the hydrogen-bond complexes of **6** increases linearly with concentration.<sup>16</sup> With a strong self-association capability, the molecules of **6** may cluster together by extruding the surrounding solvent molecules. The Leu-PA molecules may self-associate via the formation of multiple hydrogen bonds between the N-H group of one molecule and the C=O group of another, a dimeric example of which is illustrated in the upper part of Chart 2 [**6**·**6** or (**6**)<sub>2</sub>]. Upon binding to another electronegative element of oxygen, the amide proton experiences a deshielding effect, leading to the observed downfield shift in its resonance peak. Similar to that of **6**, the resonance of the amide group of **14** is also downfield shifted with an increase in concentration, but the extent of the downfield shift or the degree of the intermolecular hydrogen bonding is smaller.

To further learn the hydrogen bonding behaviors of **6**, we studied solvent effect on its NMR spectra. Methanol is a protic solvent capable of hydrogen bonding and may thus be used as a spectroscopic probe to trace the processes of intermolecular hydrogen-bond formation. Figure 3 shows the <sup>1</sup>H NMR spectra of **6** in deuterated methanol/chloroform mixtures with different methanol ratios at a fixed concentration (50 mg/mL). Addition of 20 vol % of deuteriomethanol into the deuteriochloroform solution of **6** brings about a big downfield shift in the amide resonance (cf. panels B and A of Figure 3). The shift of the amide resonance is as large as  $\delta \sim 2$  ppm when the methanol ratio is increased to 80 vol % (Figure 4). The chemical shift of the amide peak progressively increases with increasing methanol frac-

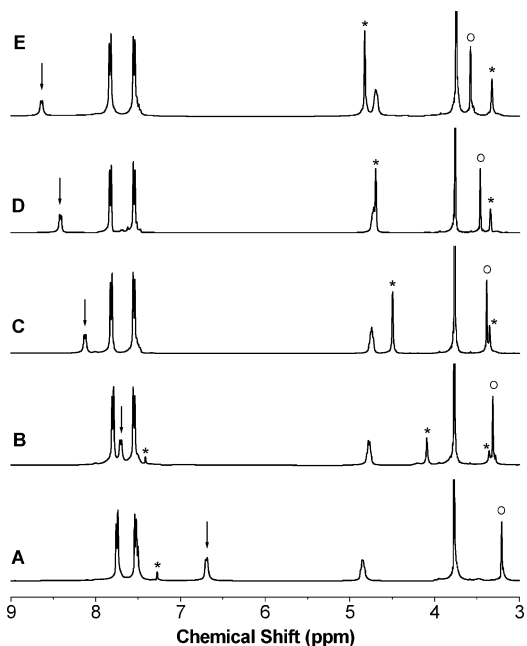


**Figure 3.** <sup>1</sup>H NMR spectra of methanol-*d*<sub>4</sub>/chloroform-*d* solutions of **6** (50 mg/mL) with varying ratios of methanol-*d*<sub>4</sub> (vol %): (A) 0, (B) 20, (C) 40, (D) 60, and (E) 80. The resonance peaks of the amide (HNCO) and ethynyl (HC≡) protons are respectively marked with downward arrows (↓) and open circles (○), while those of the solvents are marked with asterisks (\*).

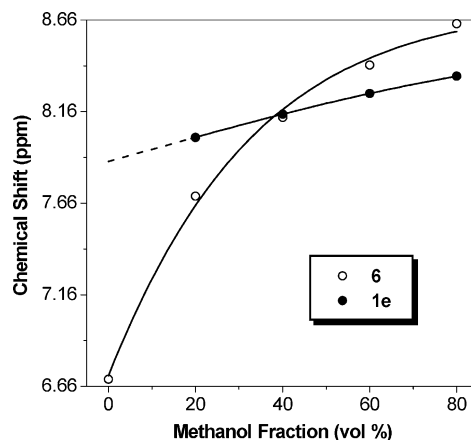


**Figure 4.** Solvent dependence of the chemical shifts of the amide resonance peaks of **6** and its polymer **1e** (sample from Table 1, no. 11) in methanol-*d*<sub>4</sub>/chloroform-*d* mixtures. Concentration: 50 mg/mL.

tion. With an increase in the methanol ratio, a particular hydrogen-bond complex will be populated and/or the number of methanol molecules complexed with one molecule of **6** ( $n$ ) will be increased (an example with  $n = 4$  being given in Chart 2), both or either of which will downfield shift the amide resonance. The formation of the intermolecular hydrogen-bond complexes is also supported by the observation that the resonance peak of the nondeuterated methanol residual is downfield shifted with an increase in the methanol ratio in the mixture (Figure 3). The heterocomplexation of the O-H group of methanol with the acidic  $\equiv C-H$  group of **6** is revealed by the downfield shift in the ethynyl resonance peak; such a shift is absent in the case of increasing the solution concentration of **6** in aprotic chloroform (cf. Figure 1).

Acetone is an aprotic but hydrogen-bonding solvent<sup>16</sup> and can also be used as a heterocomplexation probe. In

**Table 1. Polymerization of 4-Ethynylbenzoyl-L-leucine Methyl Ester (6)<sup>a</sup>**

no.	catalyst	solvent <sup>b</sup>	yield (%)	$M_w^c$	$M_w/M_n^c$	Z (%) <sup>d</sup>
1	[Rh(cod)Cl] <sub>2</sub>	DCM	23.5	148 000	8.54	97.2
2	[Rh(cod)Cl] <sub>2</sub>	DCM/TEA	89.0	613 000	3.52	84.2
3	[Rh(cod)Cl] <sub>2</sub>	THF	69.4	439 000	4.76	80.1
4	[Rh(cod)Cl] <sub>2</sub>	THF/TEA	58.2	465 000	6.95	70.6
5	[Rh(cod)Cl] <sub>2</sub>	dioxane	71.6	477 000	3.96	83.0
6	[Rh(cod)Cl] <sub>2</sub>	toluene	37.5	140 000	8.47	99.4
7	Rh(cod)(NH <sub>3</sub> )Cl	THF	59.4	632 000	3.64	100.0
8	Rh(cod)(tos)(H <sub>2</sub> O)	THF	66.6	448 000	9.02	94.9
9	Rh(cod)(tos)(H <sub>2</sub> O)	THF/TEA	86.5	590 000	8.20	89.3
10	[Rh(nbd)Cl] <sub>2</sub>	THF	78.2	1240 000	4.77	83.1
11	[Rh(nbd)Cl] <sub>2</sub>	THF/TEA	91.7	416 000 <sup>e</sup>	3.54	89.8
12	Rh(nbd)(tos)(H <sub>2</sub> O)	THF	trace			
13	Rh(nbd)(tos)(H <sub>2</sub> O)	THF/TEA	trace			

<sup>a</sup> Carried out at room temperature under nitrogen for 24 h;  $[M]_0 = 0.1$  M,  $[cat.] = 5$  mM; nbd = 2,5-norbornadiene, cod = 1,5-cyclooctadiene, tos = *p*-toluenesulfonate, TEA = triethylamine. <sup>b</sup> Volume of solvent used: 2 mL; volume of TEA added: 1 drop. <sup>c</sup> Estimated by GPC in THF on the basis of a polystyrene calibration. <sup>d</sup> Determined by <sup>1</sup>H NMR analysis. <sup>e</sup>  $M_w$  is increased to 1470 000 when  $[cat.]$  is decreased to 1 mM. [Unless otherwise stated (e.g., the hydrolysis experiments), all other measurements regarding the properties of "polyester" **1e** were carried out using the sample with  $M_w$  of 416 000.]

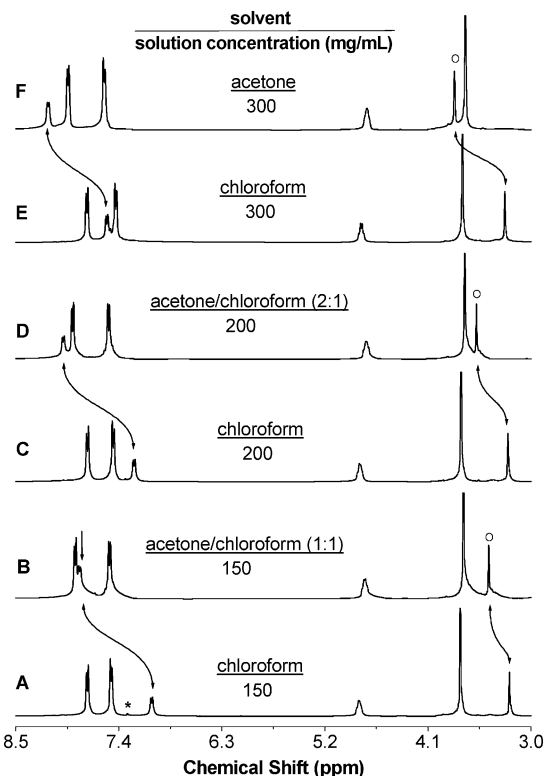


**Figure 5.** <sup>1</sup>H NMR spectra of **6** under different environmental conditions. The resonance peaks of the amide (HNCO) and ethynyl (HC≡) protons are respectively marked with downward arrows (↓) and open circles (○), while those of the solvents are marked with asterisks (\*).

deuterated acetone/chloroform mixtures, **6** exhibits a similar downfield shift with an increase in acetone ratio (Figure 5). When an equal volume of acetone (50%) is added into a chloroform solution of **6** with a concentration of 150 mg/mL, the amide resonance is downfield shifted for  $\delta \sim 0.6$  ppm. Increasing the acetone ratio to  $\sim 67\%$  and the solution concentration to 200 mg/mL further downfield shifts the amide resonance. In a concentrated solution (300 mg/mL) in "pure" acetone (100%), the amide proton of **6** resonates at a very low field (Figure 5F). This lowfield shift is obviously caused by the intermolecular hydrogen bond formation between the N-H group of **6** and the C=O group of acetone. The C=O group of the solvent also hydrogen bonds with the  $\equiv C-H$  group of **6**, giving rise to the observed large

downfield shift in the resonance peak of the ethynyl proton.

**Polymer Synthesis and Structural Characterization.** We tried to convert the Leu-PA monomers to their polymers using transition-metal catalysts. Metathesis catalysts such as WCl<sub>6</sub> and MoCl<sub>5</sub> are classic initiators for acetylene polymerization,<sup>8,17</sup> but when they were added into the monomer solutions, no polymerization occurred. Further trials with addition of cocatalysts and increase in temperature all ended up with failure. The Leu-PA adducts seem to be toxic to the metathesis catalysts, possibly due to the deactivation of the metallic species by the polar functional groups of the monomers. We then turned our attention to other transition-metal catalysts with better tolerance to polar groups. Organorhodium complexes are known to be effective in polymerizing PA monomers with functional groups in insertion mechanism,<sup>8,11,18</sup> and we thus checked whether these complexes could work for our Leu-PA monomers.

We first examined the polymerization of monomer **6** in a DCM solution of [Rh(cod)Cl]<sub>2</sub>. After 24 h reaction at room temperature, a yellowish polymeric product is isolated by precipitating the reaction mixture into an acetone/diethyl ether mixture. This proves that the rhodium complex works for the PA polymerization, although the yield of the polymer is low ( $\sim 24\%$ ; Table 1, no. 1). Addition of a small amount of triethylamine (TEA) boosts the yield of the polymer and also its  $M_w$  (to 89% and  $6.1 \times 10^5$ , respectively). The polymerizations in other solvents, including THF/TEA, dioxane, and toluene, all proceed well and give satisfactory results. We checked the ligand effect and found that, except for Rh(nbd)(tos)(H<sub>2</sub>O), all the complexes with other ligands, including Rh(cod)(NH<sub>3</sub>)Cl, Rh(cod)(tos)(H<sub>2</sub>O), and [Rh(nbd)Cl]<sub>2</sub>, functioned as effective polymerization catalysts. Particularly, when [Rh(nbd)Cl]<sub>2</sub> is used as catalyst in THF, a polymer with a remarkably high  $M_w$  ( $\sim 1.2 \times 10^6$ ) is obtained in a high yield ( $\sim 78\%$ ; Table 1, no. 10). Addition of a small amount of TEA further increased the isolation yield to  $\sim 92\%$ . When the catalyst concentration is decreased from 5 to 1 mM, a polymer with an  $M_w$  as high as  $\sim 1.5 \times 10^6$  is obtained in a comparably high yield (85.2%).

We then inspected the polymerization behaviors of **14**, a congener of **6** with a long spacer between the Leu and PA moieties. All the rhodium complexes of [Rh(cod)Cl]<sub>2</sub>, Rh(cod)(NH<sub>3</sub>)Cl, and [Rh(nbd)Cl]<sub>2</sub> are effective in poly-

**Table 2. Polymerization of 11-[(4-Ethynyl)phenoxy]undecanoyl-L-leucine Methyl Ester (14)<sup>a</sup>**

no.	catalyst	solvent <sup>b</sup>	yield (%)	$M_w^c$	$M_w/M_n^c$
1	[Rh(cod)Cl] <sub>2</sub>	THF	30.4	6000	1.74
2	[Rh(cod)Cl] <sub>2</sub>	THF/TEA	92.4	4000	5.95
3	[Rh(cod)Cl] <sub>2</sub>	DCM	40.1	3000	1.46
4	[Rh(cod)Cl] <sub>2</sub>	DCM/TEA	98.9	4000	1.69
5	Rh(cod)(NH <sub>3</sub> )Cl	THF	69.8	9000	7.69
6	Rh(cod)(NH <sub>3</sub> )Cl	DCM	63.3	18000	4.71
7	[Rh(nbd)Cl] <sub>2</sub>	THF	53.2	8000	2.19
8	[Rh(nbd)Cl] <sub>2</sub>	THF/TEA	99.0	20000	2.84
9	[Rh(nbd)Cl] <sub>2</sub>	DCM	63.6	4000	5.77
10	[Rh(nbd)Cl] <sub>2</sub>	DCM/TEA	98.2	20000	3.47
11	[Rh(nbd)Cl] <sub>2</sub>	dioxane	48.6	5000	2.88
12	[Rh(nbd)Cl] <sub>2</sub>	toluene	50.0	11000	2.28

<sup>a</sup> Carried out at room temperature under nitrogen for 24 h; [M]<sub>0</sub> = 0.1 M, [cat.] = 5 mM. *Z* contents of the polymers were not estimated by <sup>1</sup>H NMR analysis because of the difficulty in clearly identifying their amide resonance peaks in the chemical shift region of 5.5–8.0 ppm (see text). Abbreviations: nbd = 2,5-norbornadiene, cod = 1,5-cyclooctadiene, tos = *p*-toluenesulfonate, TEA = triethylamine. <sup>b</sup> Volume of solvent used: 2 mL; volume of TEA added: 1 drop. <sup>c</sup> Estimated by GPC in THF on the basis of a polystyrene calibration.

merizing this monomer. The rhodium catalyst with nbd ligand, compared to its counterparts with cod ligand, give generally better polymerization results. The polymerizations initiated by [Rh(nbd)Cl]<sub>2</sub> in THF/TEA and DCM/TEA produce polymers with high  $M_w$  (20 × 10<sup>3</sup>) in high yields (>98%; Table 2, nos. 8 and 10). Compared with those of the polymers of **6**, the molecular weights of the polymers of **14** are lower. The reason for this is not clear but may be related to the difference in the electron densities of the triple bonds of the monomers. Because of the electron-withdrawing effect of the carbonyl group (–CO–) at the para position of the phenyl ring, the ethynyl group of **6** is electron-poor, while that of **14** is electron-rich due to the electron-donating effect of the oxy (–O–) group at the same position. The electron-deficient monomer may have better coordinated with the metal center, and the resultant active species may have robustly propagated to give high molecular weight polymers.<sup>13,18c</sup> Similar phenomena have been observed in the rhodium-catalyzed polymerizations of the PA derivatives containing saccharide<sup>19</sup> and nucleoside moieties;<sup>20</sup> the monomers with the *p*-carbonyl groups produce higher molecular weight polymers than those with the *p*-oxy groups.

In the polymers of **6** and **14**, the amino acid moieties are protected by methyl ester groups, and the polymers may thus be referred to as “polyesters”, i.e., **1e** and **2e** (“e” for “ester”), respectively. We tried to cleave the methyl ester groups and convert the “polyesters” to their acid forms, “polyacids” **1a** and **2a** (“a” for “acid”), respectively. We chose KOH as the cleaving agent.<sup>21,22</sup> The base-catalyzed hydrolyses of the polyesters proceed steadily, and the deprotected polyacids are isolated in high yields (>95%). A GPC curve of the polyacid **1a** obtained after ~1 h hydrolysis of **1e** is shown in Figure 6 as an example. The chromatogram is “normal” in shape, from which an  $M_w$  of ~1.1 × 10<sup>6</sup> is estimated. The high  $M_w$  value proves that the polymer has not undergone catastrophic decomposition during the hydrolysis reaction because one or two backbone scissions would dramatically decrease the  $M_w$  to half or one-third of its original value. The  $M_w$  value of the polyacid is somewhat lower than that of the starting polyester

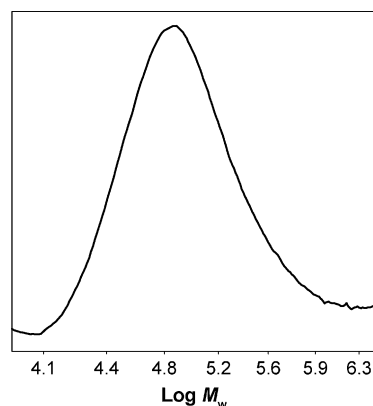


**Figure 6.** GPC chromatogram of **1a** prepared by ~1 h hydrolysis of **1e** (sample from Table 1, no. 11, note e) in methanol at room temperature.

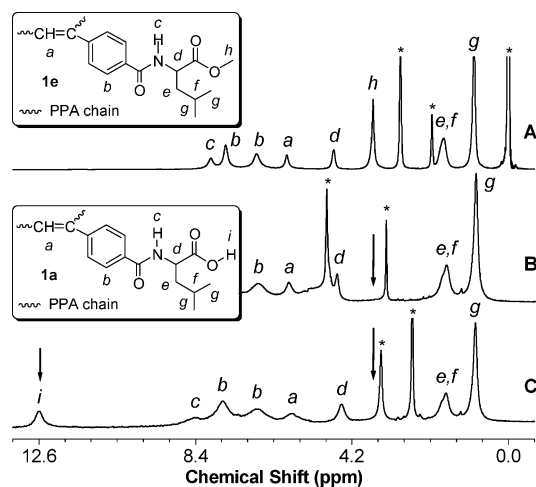
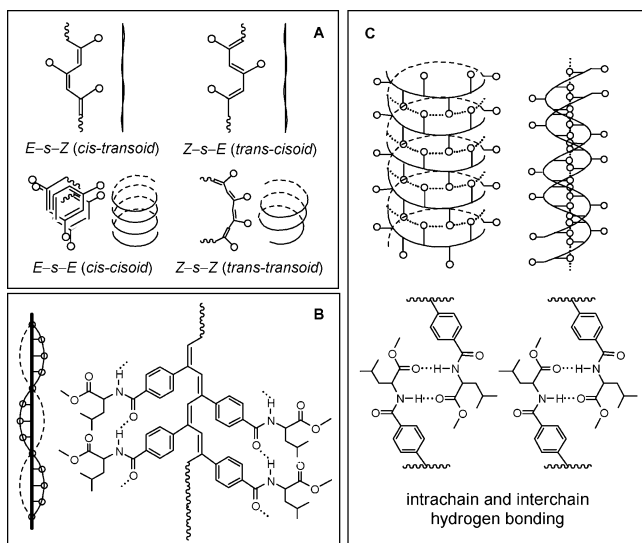


**Figure 7.** <sup>1</sup>H NMR spectra of (A) acetone-*d*<sub>6</sub> solution of **1e** (sample from Table 1, no. 11) and (B) methanol-*d*<sub>4</sub> and (C) DMSO-*d*<sub>6</sub> solutions of **1a** (sample from Figure 6). The resonance peaks of TMS, solvents, and water are marked with asterisks (\*).

(~1.5 × 10<sup>6</sup>), partly because of the cleavage of the methyl ester groups of the pendants and probably also due to the different solubility and hence hydrodynamic volume of the polyacid from that of the polyester parent in the eluent. Interestingly, prolongation of the hydrolysis time to 2 h brings about little change in the isolation yield and molecular weight of the resultant polyacid, suggesting that the hydrolysis reaction is mild and harmless to other functional groups of the polymer. Similar results are obtained when the Leu groups of **2e** are deprotected by the KOH-catalyzed hydrolysis under similar reaction conditions.

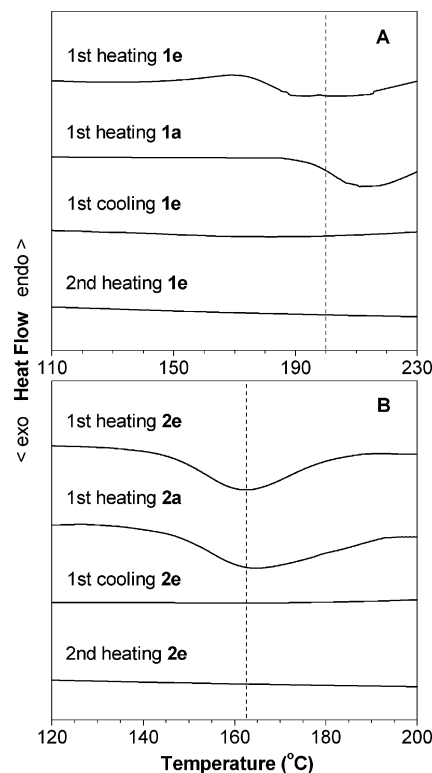
We used spectroscopic methods to analyze the molecular structures of the polymers (see Experimental Section for detailed characterization data). An example of the <sup>1</sup>H NMR spectra of polyacid **1a** is shown in Figure 7; a spectrum of its polyester parent **1e** is also given in the same figure for the purpose of comparison. Polyester **1e** shows a well-resolved spectrum in deuterioacetone, well corresponding to its expected molecular structure. The resonance of the protons of its ester (CO<sub>2</sub>CH<sub>3</sub>), vinyl (HC≡), and amide (HNCO) groups peak at δ ~3.8, ~5.9, and ~8.0, respectively (Figure 7A). After hydrolysis, the polyacid product exhibits no any ester signals at δ ~3.8 (Figure 7B), in place of which a new acid peak appears at δ ~12.6 (Figure 7C). The vinyl and amide peaks remain intact. The spectroscopic data thus con-

Chart 3



firm that the methyl ester groups have been completely cleaved and that the double bonds in the PPA backbone and the amide bonds in the Leu pendants have been unharmed by the KOH-catalyzed deprotection reaction. It is well-known that an ester bond is much easier to undergo hydrolysis reaction than an amide bond,<sup>21,22</sup> and this reactivity difference enabled us to selectively hydrolyze the ester groups under the mild reaction conditions.

For a PPA derivative, there exist four theoretically possible stereostructures of chain segments: *E-s-Z*, *Z-s-E*, *E-s-E*, and *Z-s-Z*, which are conventionally named as *cis-transoid*, *trans-cisoid*, *cis-cisoid*, and *trans-transoid*, respectively (Chart 3A).<sup>23,24</sup> The ease of the formation of a certain conformational structure is mainly determined by the steric and electronic effects of the pendant groups (*o*). The PA polymerization may produce the chain segments of *E-s-Z* and *Z-s-E* conformations, and the formation of the *E-s-E* and *Z-s-Z* conformers is unlikely because of the obvious unfavorable steric effect.<sup>23,24</sup> The *E-s-Z* and *Z-s-E* segments should resonate at different frequencies in the NMR analysis because they locate in different chemical environments: indeed, calculations on the basis of Shoolery's rules suggest that the *E-s-Z* and *Z-s-E* conformers of PPA absorb at  $\delta$  6.36 and 6.09, respectively. Polyester **1e**, being a PPA derivative, shows a singlet centered at  $\delta \sim 5.8$  (cf. Figure 7A), which is thus assignable to the resonance of the olefinic proton of the *Z-s-E* conformer of the polymer. Using an equation similar to those we published previously,<sup>18,23</sup> the *Z* content of **1e** is estimated to be  $\sim 90\%$  (cf. Table 1, no. 11). The polymers prepared under other conditions are all *Z*-rich, with the polymer prepared by Rh(cod)-(NH<sub>3</sub>)Cl in THF exhibiting a *Z* content of 100% (Table 1, no. 7); that is to say, the polymer possesses a perfectly stereoregular *Z* conformation. Similarly, from the NMR spectrum of polyacid **1a**, it is estimated that its *Z* content is  $\sim 90\%$ , identical (within experimental error) to that of the starting material, viz., its polyester parent **1e**. This provides circumstantial evidence that the polymer backbone is unbroken and that the chain stereoregularity is unaffected by the base-catalyzed hydrolysis reaction.



**Figure 8.** DSC thermograms of (A) **1e** (Table 1, no. 11) and **1a** (prepared by  $\sim 1$  h hydrolysis of **1e**) and (B) **2e** (Table 2, no. 8) and **2a** (prepared by  $\sim 1$  h hydrolysis of **2e**) recorded during heating and cooling scans under nitrogen at a scanning rate of  $10^\circ\text{C}/\text{min}$ .

The similar calculation of *Z* content, however, cannot be done for polyester **2e**. Its NMR spectra in deuterated chloroform and DCM are poorly resolved. The resonance peak of its amide proton cannot be identified and resolved with confidence because of its overlapping with those of the aromatic and olefinic protons in the chemical shift region of  $\delta$  5.5–8.0. Fortunately, polyacid **2a** gives a resolved spectrum in methanol-*d*<sub>4</sub>, from which a *Z* content of  $\sim 81\%$  is obtained. This high *Z* content suggests that **2a** possesses a stereoregular conformation. As discussed above, in the case of polymers **1**, the PPA chain conformation is unaffected by the hydrolysis reaction. The same may be true for polymers **2**: the chain conformation of polyester **2e** may also be stereoregular and *Z*-rich because its polyacid cousin **2a** possesses a high *Z* content.

It is well-known that (unsubstituted) polyacetylene  $-(\text{CH}=\text{CH})_n-$  undergoes irreversible *cis-to-trans* isomerization upon thermal treatment.<sup>25</sup> Being polyacetylene derivatives, **1** and **2** may also isomerize from *Z* to *E* conformation when a sufficient amount of energy is supplied. We thus used differential scanning calorimetry (DSC) to investigate their isomerization processes. In the first heating scan, **1e** starts to exhibit an exothermic valley from  $\sim 170^\circ\text{C}$  (Figure 8A). Thermogravimetric analysis (TGA) indicates that **1e** is thermally stable and does not lose any weight when heated to a temperature as high as  $\sim 260^\circ\text{C}$ . The exothermic valley around  $200^\circ\text{C}$  should thus be associated with its thermally induced *Z-E* isomerization. Like that of its polyacetylene parent, the isomerization of **1e** is also irreversible: the successive first cooling and second heating scans detect no any peaks at  $\sim 200^\circ\text{C}$  and give almost flat lines over the whole scanned temperature region. Polyacid **1a** exhibits a similar exothermic valley but in a higher

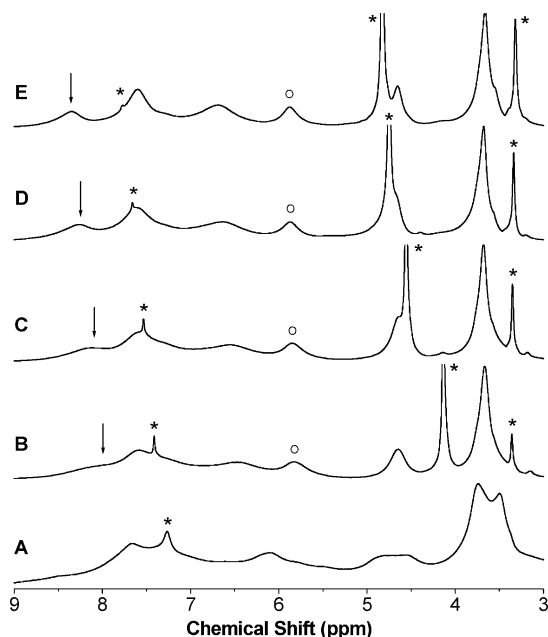


**Figure 9.**  $^1\text{H}$  NMR spectra of methanol- $d_4$ /chloroform- $d_3$  solutions of **1e** (50 mg/mL; sample from Table 1, no. 11) with varying ratios of methanol- $d_4$  (vol %): (A) 0, (B) 20, (C) 40, (D) 60, and (E) 80. The resonance peaks of the amide (HNCO) and vinyl (HC=) protons are respectively marked with downward arrows (↓) and open circles (○), while those of the solvents are marked with asterisks (\*).

temperature region. The multiple hydrogen bonding between the polyacid strands may have rigidified the macromolecular chains, thus “red”-shifting the isomerization temperature.<sup>26</sup>

Similar phenomena are observed in the DSC analyses of **2**. Although some technical difficulties are encountered in directly determining the *Z* content of **2e**, the polyester exhibits an exothermic peak associated with *Z*–*E* isomerization in the first heating scan (Figure 8B), proving that **2e** is indeed *Z*-rich in conformation. Compared to **1e**, **2e** undergoes isomerization in a lower temperature region, which may be caused by the internal plasticization effect of its long flexible spacer. The isomerization is again irreversible, as verified by the virtually flat lines recorded by DSC during the first cooling and second heating scans. The isomerization temperature of polyacid **2a** is, however, only slightly higher than that of its polyester parent **2e**. The stiffness of the polyene backbone of **2a** is probably affected to a little extent by the hydrogen bonding between the Leu pendants because of the decoupling effect of the flexible alkyl buffer between the main and side chains.

**Molecular Interaction and Chain Helicity.** The  $^1\text{H}$  NMR analyses of the Leu–PA adducts offered useful information about the intra- and intermolecular hydrogen bonding of the monomers (cf. Figures 1–5), and we used the same technique to investigate the molecular interactions in their polymers. The high molecular weights of the polymers made their solutions very viscous, leaving little room for us to manipulate in terms of varying their solution concentrations. We were, however, able to examine the solvent effect, although the high molecular weights of the polymers significantly limited our choice of solvent. Figure 9 shows the  $^1\text{H}$  NMR spectra of **1e** in deuterated methanol/chloroform mixtures. The spectrum in “pure” chloroform is broad, possibly due to association of the macromolecular chains in the nonpolar solvent through intra- and interchain

hydrogen bonding.<sup>27</sup> The poor resolution of the spectrum makes it difficult to elucidate the resonance signals. Addition of a small amount of methanol (20 vol %) to the chloroform solution helps improve the spectral resolution, and the amide resonance can now be identified to occur at  $\delta \sim 8$  (Figure 9B). Further addition of more methanol solvent progressively downfield shifts the resonance peak of the amide proton as well as that of the hydroxyl proton of methanol solvent. Clearly, intermolecular hydrogen bonds have been formed between the hydroxyl groups of the solvent molecules and the amide groups of the Leu pendants. Such hydrogen bonding should contribute to the solvation of the polymer chains and to the partial disassembling of the self-associated macromolecular clusters, making the polymer more soluble and the spectra better resolved.

When the NMR data are plotted, the change in the solvent composition is found to cause relatively small downfield shift in the amide resonance of the polymer, in comparison to that of its monomer (Figure 4). The smaller changes in chemical shift and the broader peaks of proton resonance are attributable to the existence of the intra- and interstrand hydrogen bonds in the polymer system, as schematically illustrated in panels B and C of Chart 3. When the Leu moieties are covalently bound to every repeat unit of the PPA chain, the closely located amide groups in the same and/or different chains may readily form hydrogen bonds in relatively nonpolar environment, which may explain why the amide resonance of the polymer is more downfield shifted than that of its monomer in the solvent mixture with a low methanol fraction (cf. Figure 4). The steric effect of the macromolecular chain, on the other hand, may hamper the methanol molecules from approaching the amide groups of the Leu pendants; as a consequence, not all the amide groups can form intermolecular hydrogen bonds with the solvent molecules. This may thus explain why the extents of the downfield shifts of the amide resonance of the polymer are smaller than those of its monomer in the solvent mixtures with high methanol fractions.

Also because of steric reasons, bulky pendants of neighboring repeat units of the polymers may not be able to locate on the same plane but have to twist an angle to avoid the involved steric crowdedness. When the pendants are asymmetric, their cooperative twisting toward one preferred direction may generate a chiral force field to induce the chain segments to spiral in a crew sense. To get some clues on whether the PPA chains are induced to helically rotate, we measured their optical rotations at 20 °C ( $[\alpha]_D^{20}$ ). In toluene, polyester **1e** showed an  $[\alpha]_D^{20}$  value as high as  $-826.1^\circ$  (Table 3, no. 1), which is opposite in sign and bigger in magnitude compared to that of its monomer ( $+23.4^\circ$ ). It is known that a polymer chain with a helical conformation can generate a very high optical activity,<sup>4</sup> and the high  $[\alpha]_D^{20}$  value of **1e** suggests that its optical activity is not from its chiral Leu pendants but from its helical PPA chains. Interestingly, the  $[\alpha]_D^{20}$  value of the polyester varies drastically with solvent; that is, its optical activity is susceptible to the surrounding environment. When the solvent changes from toluene to chloroform and finally to DMF, the  $[\alpha]_D^{20}$  value changes in magnitude and/or sign (from  $-826.1^\circ$  to  $-737.7^\circ$  and finally to  $+183.3^\circ$ ; Table 3, nos. 1–5). Polyacid **1a** exhibits similar  $[\alpha]_D^{20}$  values, which also varies vigorously with solvent. There seemingly exists some correlation between the Debye

**Table 3. Specific Rotations of L-Leucine-Containing Poly(phenylacetylene)s in Different Solvents**

no.	solvent	$(\epsilon - 1)/(\epsilon + 2)^a$	$[\alpha]_D^{20}$ , deg (c, g/dL)	
			<b>1e</b>	<b>1a<sup>b</sup></b>
1	toluene	0.31	-826.1 (0.092)	
2	chloroform	0.56	-737.7 (0.132)	-606.7 (0.045) <sup>c</sup>
3	DCM	0.73	-394.7 (0.064)	
4	methanol	0.91	-101.2 (0.082)	-197.1 (0.034)
5	DMF	0.92	+183.3 (0.036)	+323.4 (0.047)
			<b>2e</b>	<b>2a<sup>b</sup></b>
6	chloroform	0.56	~0.0 (0.500)	
7	water	0.96		~0.0 (0.300) <sup>d</sup>

<sup>a</sup> Debye solvent polarizability function.<sup>28</sup> <sup>b</sup> Prepared by ~1 h hydrolyses of **1e** (Figure 6) or **2e** (Figure 8B). <sup>c</sup> Mixture of methanol/chloroform (3:7 by volume) used in this measurement. <sup>d</sup> Alkalified with NaOH (0.2 M)

solvent polarizability and the specific optical rotation, with both **1e** and **1a** displaying highest  $|\alpha]_D^{20}|$  values in nonpolar solvents.

Polymers **2**, however, behave in a very different way. Polyester **2e** shows a nearly zero  $[\alpha]_D^{20}$  value in chloroform (Table 3, no. 6). Similarly, polyacid **2a** is optically inactive, whose  $[\alpha]_D^{20}$  value in alkalified water is practically nil. We checked the solvent effects of the polymers but failed to obtain high  $[\alpha]_D^{20}$  values, although small optical activities are observed in a few solvent mixtures (e.g.,  $[\alpha]_D^{20}$  values of +75° and +45° are obtained for **2e** in the chloroform/methanol mixtures with 1:7 and 1:11 volume ratios, respectively). On the basis of these observations, it may be concluded that polymers **2** do not possess helical structures with a predominant handedness. This suggests that the stereogenic Leu moieties located far apart from the conjugated PPA backbone cannot effectively induce the main chain to helically rotate or that the relaxation of the long flexible alkyl spacers has virtually shut off the chiral transmission process from the Leu pendants to the PPA backbone. On the other hand, the Leu moieties in polymers **1** are linked to the PPA backbone via rigid aromatic connecting groups, which may have enabled efficient transcription of the pendant chirality to the backbone helicity. As discussed above, the high optical activities of **1** suggest that the polymers possess helical conformations, and we thus further studied their chiroptical properties using circular dichroism (CD) spectropolarimetry, a powerful tool for conformational analysis.<sup>29,30</sup>

As shown in the upper part of Figure 10, polymer **1e** is clearly CD-active. In chloroform, it exhibits a strong CD band at ~375 nm with a molar ellipticity ( $[\theta]$ ) as high as ca. -43 800 deg cm<sup>2</sup> dmol<sup>-1</sup>. Since its monomer **6** is CD-inactive at  $\lambda > 300$  nm, the first Cotton effect of the polymer (at ~375 nm) thus must be associated with the absorption of its conjugated PPA backbone, proving that the polymer chains take helical conformations with an excess of one-handedness. The high CD intensity or strong Cotton effect implies a great predominance of the chain segments with long persistence lengths of one helical sense. While the formation of regular chains of helical conformation is entropically unfavorable, this entropic cost may be compensated or balanced by the stabilization effects of intra- and/or interstrand hydrogen bonds formed between the Leu moieties, as diagrammatically depicted in panels B and C of Chart 3. This balance may, however, be readily broken by external perturbations, taking into account the noncovalent nature of the hydrogen bonding, and

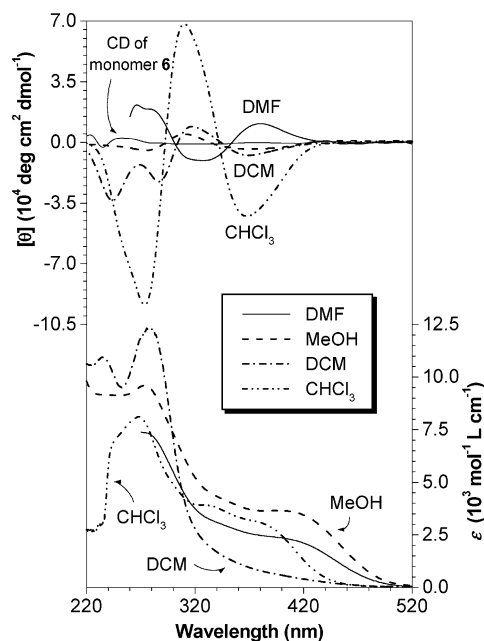


**Figure 10.** CD and UV spectra of **1e** (sample from Table 1, no. 11) in different solvent environments. CD spectrum of a chloroform solution of monomer **6** is shown for comparison. Spectral data in DMF below 260 nm were not taken because of the interference by solvent absorption. Concentration (mM): ~1.5 (CD), ~0.1–0.3 (UV).

the system may adapt to the new environments and reach new equilibrium states under the new sets of external conditions. Careful examination of the four conformational structures shown in Chart 3A reveals that the handedness and pitch of a helical segment of a PPA chain can be altered through a single-bond rotation. Such an atropisomeric transition involves little energy,<sup>4</sup> thus further suggesting a high susceptibility of the chain helicity to external perturbations. Indeed, the CD spectrum of **1e** is very sensitive to a change in its environment. Similar to its  $[\alpha]_D^{20}$ , the  $[\theta]$  of the polymer changes markedly with solvent, a “simple” external perturbation. The intensities of the CD peaks are considerably weakened, when the solvent is changed from chloroform to DCM and methanol. In DMF, the first Cotton effect is inverted in sign, suggesting that the relative population of the right- and left-handed helical chains in this solvent is opposite to those in other solvents.

It is envisioned that the PPA chains of different conformations may undergo different electronic transitions. This is indeed the case and **1e** exhibits solvatochromism:<sup>31</sup> its absorption spectrum changes with solvent. In DCM, **1e** absorbs little visible light (lower part of Figure 10). In a related chiral poly(propargyl) system, it was found that the polyacetylenes capable and incapable of absorbing visible light possessed helical and disordered conformations, respectively.<sup>32</sup> The same may be true for **1e**. Its low absorptivity in the visible suggests that its PPA backbone is not well conjugated, due possibly to the irregular bending and crumpling of the polymer chains in this solvent of middle polarity (cf. Table 3, no. 3). Such disordered PPA chains may coil in a random fashion and hence exhibit little CD activity in the visible. Chloroform possesses a low Debye solvent polarizability. The polymer chains may self-associate in this nonpolar solvent, as suggested by the poorly resolved NMR spectrum of **1e** in deuteriochloroform (cf. Figure 9A). In the self-association process, the helical

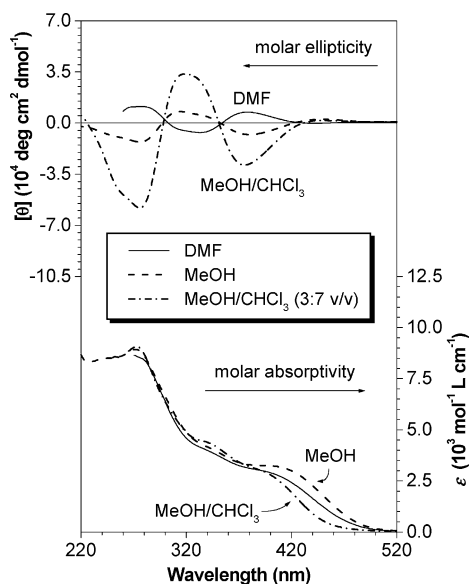


**Figure 11.** CD and UV spectra of **1a** (sample prepared by ~45 min hydrolysis of **1e**) in different solvent environments. Spectral data in DMF below 260 nm were not taken because of the interference by the solvent absorption. Polymer concentration (mM): ~1.5 (CD), 0.1–0.2 (UV).

segments may act as chaperons<sup>1</sup> to guide the polymer chains to fold into regular superhelix structures.<sup>30</sup> The “sergeant and soldier” principle<sup>33</sup> may also come into play: the chiral segments may serve as templates to correct the misarranged segments via cooperative hydrogen bonding. The resultant supramolecular assemblies with regular chain helicity are probably responsible for the strong Cotton effects of the polymer in chloroform.<sup>30</sup> DMF, on the other hand, is a polar solvent with a high solvating power. The solvated polymer chains may take extended conformations with long persistence lengths of conjugation, hence the observed high absorptivity in the visible spectral region. The specific solvent–chain interactions may have inverted the predominance of the chain segments of one-handedness over the other, thus reversing the sign of the first Cotton effect, compared to those in other solvents. The solvating power of protic methanol to the Leu pendants is even higher. When the solvating interaction becomes so strong, it effectively increases the bulkiness of the pendant groups. According to Grubbs and co-workers, such steric effects may force the PPA backbone to take more conjugated conformation<sup>17b</sup> and to absorb more strongly in the visible. The strong hydrogen bonding of methanol with the Leu moiety (cf. Chart 2) may, however, destroy the intra- and interchain hydrogen bonds (cf. Chart 3). Without stabilization by the self-associating hydrogen bonds, entropic chaos may randomize the rotating directions of the chain segments. The polymer chain consisting of randomly rotating segments without a strong preference of one-handedness thus shows weak CD signals. The hypothesis of strong solvation of the polymer chains by methanol is substantiated by the well-resolved <sup>1</sup>H NMR spectrum of **1e** in deuteriomethanol (see Supporting Information). Not only the Leu pendant but also the PPA backbone show sharp resonance peaks—this is possible only when both the pendant and the backbone are well solvated by, or exposed to, the solvent; in other words, the polymer chains are molecularly dissolved without aggregation. The isolated polymer strands, in the absence of the regulating and stabilizing intra- and interchain hydro-

gen bonds, would be randomized to irregular conformations without a strong preference in chain helicity.

Polyacid **1a** exhibits chiroptical properties similar to those of its polyester counterpart **1e**. Again, **1a** shows opposite helical preponderance of chain segments in DMF and methanol (Figure 11). Adding nonpolar solvent of chloroform into polar solvent of methanol enhances its Cotton effects, probably due to the formation of regular superhelix structures in the solvent mixture with relatively low polarity. The absorption spectra of **1a** are also similar to those of **1e**. No marked solvatochromism is, however, observed in this system; the polyacid is only partially soluble in nonpolar solvents, which prevented us from using the solvents with appreciably different polarizabilities. As for polymers **2e** and **2a** with long alkyl spacers between the Leu pendants and the PPA backbone, almost no CD signals are detectable at  $\lambda > 300$  nm in all the solvents we tested, doubly confirming the nonhelicity of macromolecular chains of this group of polymers.

### Concluding Remarks

In this work, we melded a naturally occurring building block, L-leucine, with a synthetic conjugated polymer, polyacetylene, and generated the hybrid amphiphilic polymers encoded with pendant chirality and hydrogen-binding capability. Our results and findings can be summarized as follows:

(1) *Molecular hybridization*: We successfully created the stereoregular Leu–PPA molecular hybrids and converted the polyesters to their corresponding polyacids by selective hydrolyses without harming the amide functional groups.

(2) *Z–E isomerization*: The chain conformations of the polymers are isomerized by a simple thermal process: heating the polymers to ~160–200 °C readily changes the *Z* conformers to their *E* isomers.

(3) *Hydrogen bonding*: The <sup>1</sup>H NMR analyses offer direct experimental evidences for the existence of intra- and interchain hydrogen bonds in the polymer systems, and the CD and UV analyses reveal their involvements in the induction and stabilization of the (supra)molecular helical structures.

(4) *Chain helicity*: The chain segments of the polyene backbones are induced by the chiral pendants to helically spiral in a screw sense. The pendant chirality–backbone helicity transcription process is, however, essentially turned off by placing the chiral pendants far apart from the polyene backbone.

(5) *Solvatochromism*: Electronic absorptions and chiroptical transitions of the polyacetylene solutions are altered to considerable extents by varying their solvents.

We are currently studying the hierarchical assembly and biological activity of the new amphiphilic helical polymers. Our preliminary microscopic and bioassay results indicate that the hybrid polymers readily self-fold into biomimetic nanostructures<sup>34</sup> and are cyto-compatible when placed in contact with living cells.<sup>35</sup> The results of our systematic investigations on the supramolecular self-organizations and biomedical applications of the polymers will be reported in due course.

### Experimental Section

**Materials.** Dioxane, toluene, and THF were purchased from Aldrich, dried over 4 Å molecular sieves, and distilled from sodium benzophenone ketyl immediately prior to use. DCM (Lab-scan) and DMF (RdH) were distilled over calcium hy-

dride. TEA and pyridine (both RdH) were distilled and dried over KOH. Acetone (Lab-scan) and DMSO (Merck) were dried over 4 Å molecular sieves prior to use. L-Leucine methyl ester hydrochloride (**5**;  $[\alpha]_D^{24} +13.2^\circ$  (*c* 5, H<sub>2</sub>O); Sigma), 11-bromoundecanoic acid (**7**), 4-iodophenol (**9**), (trimethylsilyl)acetylene (**11**), bis(triphenylphosphine)palladium(II) chloride, DCC, DMAP, copper(I) iodide (all Aldrich), methanol (Lab-scan), thionyl chloride, potassium iodide, and potassium hydroxide (all RdH) were used as received. 4-Ethynylbenzoic acid (**3**) and the rhodium complexes were prepared according to our previously described procedures.<sup>13,36</sup>

**Instrumentation.** The average molecular weights ( $M_w$  and  $M_n$ ) and polydispersity indexes ( $M_w/M_n$ ) of the polymers were estimated by GPC using a Waters Associates liquid chromatograph equipped with a Water 510 HPLC pump, a column temperature controller, a Waters 486 wavelength-tunable UV detector, and a Waters 410 differential refractometer. Styragel columns HT3, HT4, and HT6 were used in the GPC system, covering a molecular weight range as wide as  $10^2$ – $10^7$ . The polymer solutions were prepared in THF (~2 mg/mL) and filtered with 0.45 μm PTFE syringe-type filters before being injected into the GPC system. THF was used as eluent at a flow rate of 1.0 mL/min. The column temperature was maintained at 40 °C, and the working wavelength of the UV detector was set at 254 nm. A set of 12 monodisperse polystyrenes (Waters) was used as calibration standards.

The FT-IR spectra were recorded on a Perkin-Elmer 16 PC FT-IR spectrometer. The <sup>1</sup>H and <sup>13</sup>C NMR spectra were measured on a Bruker ARX 300 NMR spectrometer in deuterated solvents of chloroform-*d*, acetone-*d*<sub>6</sub>, DCM-*d*<sub>2</sub>, methanol-*d*<sub>4</sub>, and/or DMSO-*d*<sub>6</sub>. The solvents and tetramethylsilane (TMS) were used as internal references for the NMR analyses. The thermal stability of the polymers was evaluated on a Perkin-Elmer TGA 7 under nitrogen at a heating rate of 10 °C/min. The DSC thermograms of the polymers were recorded on a Setaram DSC 92 under nitrogen at a scanning rate of 10 °C/min. The UV spectra were recorded on a Milton Roy Spectronic 3000 array spectrophotometer. The specific optical rotations ( $[\alpha]_D^{20}$ ) were measured on a Perkin-Elmer 241 polarimeter at 20 °C using a beam of plane-polarized light of *d* line of a sodium lamp (589.3 nm) as monochromatic source. The CD spectra were taken on a Jasco J-720 spectropolarimeter in 1 mm quartz cuvettes using a step resolution of 0.2 nm, a scan speed of 50 nm/min, a sensitivity of 0.1°, and a response time of 0.5 s. Each spectrum was the average of 5–10 scans. The molar concentrations of the polymer solutions were calculated on the basis of the repeat units of the polymers.

**Monomer Synthesis.** The chiral Leu-PA adducts **6** and **14** were prepared by amidations of 4-ethynylbenzoyl chloride **4** and 11-[(4-ethynyl)phenoxy]undecanoic acid **13**, respectively, with L-leucine methyl ester hydrochloride **5** (cf. Schemes 1 and 2). The detailed experimental procedures are given below.

**4-Ethynylbenzoyl Chloride (4).** Into a 100 mL, two-necked round-bottom flask were added 1 g (6.8 mmol) of **3** and 10 mL of DCM under nitrogen. After cooling with an ice-water bath, 0.8 mL (11 mmol) of thionyl chloride and 0.1 mL of DMF were slowly injected into the flask. The resultant mixture was slowly warmed to room temperature and stirred for ~8 h (or until the acid completely dissolved). Excess thionyl chloride and solvent were removed at 40 °C under reduced pressure. The pure acid chloride was obtained by extraction with diethyl ether (50 mL × 3). Evaporation of the solvent gave 0.92 g of pale orange crystals of **4** (yield: 82.2%). IR (KBr),  $\nu$  (cm<sup>-1</sup>): 2364 (s, ≡C-H), 2110 (s, C≡C), 1728 (s, C=O). <sup>1</sup>H NMR (300 MHz, CDCl<sub>3</sub>),  $\delta$  (TMS, ppm): 8.1 (m, 2H, aromatic protons *o* to C=O), 7.6 (m, 2H, aromatic protons *m* to C=O), 3.4 (s, 1H, ≡CH).

**4-Ethynylbenzoyl-L-leucine Methyl Ester (6).** Into a 100 mL round-bottom flask were added 1.11 g (6.1 mmol) of **5**, 3 mL of pyridine, and 10 mL of DCM under nitrogen. The contents were mixed by stirring and then cooled with an ice bath. A solution of **4** (1.00 g, 6.1 mmol) in 10 mL of DCM was slowly injected into the flask. The reaction mixture was gradually warmed to room temperature and stirred overnight. The mixture was diluted with 100 mL of DCM, and the resultant

solution was washed twice with a dilute hydrochloric acid solution and once with deionized water. The organic layer was dried over 5 g of magnesium sulfate. After filtration of the solid and removal of the solvent, the crude product was purified on a silica gel column using a mixture of chloroform/acetone (15:1 by volume) as eluent. Evaporation of the solvents gave 1.12 g of **6** as white solid (yield: 67.1%). IR (KBr),  $\nu$  (cm<sup>-1</sup>): 2105 (m, C≡C), 1742 (s, C=O), 1628 (s, C=O). <sup>1</sup>H NMR (300 MHz, CDCl<sub>3</sub>),  $\delta$  (TMS, ppm): 7.8 (m, 2H, aromatic protons *o* to C=O), 7.5 (m, 2H, aromatic protons *m* to C=O), 6.6 (d, 1H, NH), 4.8 (m, 1H, NHCH), 3.8 (s, 3H, CO<sub>2</sub>CH<sub>3</sub>), 3.2 (s, 1H, ≡CH), 1.7 (m, 3H, CHCH<sub>2</sub>), 1.0 (m, 6H, (CH<sub>3</sub>)<sub>2</sub>). <sup>13</sup>C NMR (75 MHz, CDCl<sub>3</sub>),  $\delta$  (CDCl<sub>3</sub>, ppm): 173.7 (CO<sub>2</sub>), 166.3 (CONH), 133.7 (aromatic carbon attached to C=O), 132.1 (aromatic carbons *m* to C=O), 127.0 (aromatic carbons *o* to C=O), 125.5 (aromatic carbon *p* to C=O), 82.7 (PhC≡), 79.6 (HC≡), 52.4 (CO<sub>2</sub>CH<sub>3</sub>), 51.1 (NHCH), 41.5 (CH<sub>2</sub>), 24.9 (CH), 22.8, 21.9 ((CH<sub>3</sub>)<sub>2</sub>).  $[\alpha]_D^{20} +23.4^\circ$  (*c* 0.064, chloroform).

**Methyl 11-Bromoundecanoate (8).** Into a 500 mL round-bottom flask equipped with a reflux condenser were added **7** (13.3 g, 50 mmol) and 200 mL of methanol. With gentle stirring, 5 mL of concentrated sulfuric acid was added dropwise into the flask. The reaction mixture was refluxed for 2 h. After cooling the content to room temperature, calcium carbonate was added gradually to neutralize the excess acid. The solvent was removed by a rotary evaporator. The residue in the flask was redissolved in 200 mL of chloroform and washed with deionized water. The organic layer was dried over 5 g of magnesium sulfate. After filtration of the solids and removal of the solvent, the crude product was purified on a silica gel chromatography column using chloroform as eluent. Evaporation of the solvent afforded 11.9 g of **8** as colorless liquid (yield: 85.2%). <sup>1</sup>H NMR (300 MHz, CDCl<sub>3</sub>),  $\delta$  (TMS, ppm): 3.7 (s, 3H, OCH<sub>3</sub>), 3.4 (m, 2H, CH<sub>2</sub>Br), 2.3 (m, 2H, CH<sub>2</sub>CO<sub>2</sub>CH<sub>3</sub>), 1.9 (m, 2H, CH<sub>2</sub>CH<sub>2</sub>Br), 1.6 (m, 2H, CH<sub>2</sub>CH<sub>2</sub>CO<sub>2</sub>CH<sub>3</sub>), 1.5–1.3 (m, 12H, (CH<sub>2</sub>)<sub>6</sub>).

**Methyl 11-(4-Iodophenoxy)undecanoate (10).** Into a 250 mL round-bottom flask equipped with a reflux condenser, 5 g (22.7 mmol) of **9**, 1.3 g (23.2 mmol) of potassium hydroxide, and 5.7 g (34.3 mmol) of potassium iodide were dissolved in 100 mL of acetone/DMSO (9:1, v/v) mixture with gentle stirring. To the mixture was added 6.3 g (22.6 mmol) of **8**, and the content was then refluxed for 24 h. The solids were removed by filtration, and the filtrate was evaporated under reduced pressure. The crude product was dissolved in 50 mL of DCM, and the resultant solution was washed with 50 mL of deionized water. The aqueous phase was extracted twice with 50 mL of DCM. The combined organic layers were dried over 5 g of magnesium sulfate. The crude product was condensed and purified on a silica gel column using chloroform as eluent. Evaporation of the solvent gave 7.5 g of pale yellow solid of **10** (yield: 79.3%). <sup>1</sup>H NMR (300 MHz, CDCl<sub>3</sub>),  $\delta$  (TMS, ppm): 7.5 (m, 2H, aromatic protons *m* to -O-), 6.7 (m, 2H, aromatic protons *o* to -O-), 3.9 (m, 2H, PhOCH<sub>2</sub>), 3.7 (s, 3H, OCH<sub>3</sub>), 2.3 (m, 2H, CH<sub>2</sub>CO<sub>2</sub>CH<sub>3</sub>), 1.8 (m, 2H, PhOCH<sub>2</sub>CH<sub>2</sub>), 1.6 (m, 2H, CH<sub>2</sub>CH<sub>2</sub>CO<sub>2</sub>CH<sub>3</sub>), 1.5–1.3 (m, 12H, (CH<sub>2</sub>)<sub>6</sub>).

**Methyl 11-[(4-Trimethylsilylethynyl)phenoxy]undecanoate (12).** Into a 100 mL, two-necked, round-bottom flask were added 140 mg (0.2 mmol) of bis(triphenylphosphine)palladium(II) chloride, 10 mg (0.05 mmol) of copper(I) iodide, and 40 mL of a TEA solution of **10** (4.18 g, 10 mmol) under nitrogen. After all the catalysts were dissolved, 1.7 mL (12 mmol) of **11** was injected into the flask, and the mixture was stirred at room temperature for 12 h. The solids formed during the reaction were removed by filtration and washed with TEA. The filtrate was then evaporated by a rotary evaporator. The residue in the flask was redissolved in 100 mL of chloroform and washed with 50 mL of hydrochloric acid (1 M) and then 50 mL of deionized water. The crude product was condensed and purified on a silica gel column using chloroform as eluent. Removal of the solvent gave 3.6 g of light yellow solid of **12** (yield: 92.7%). IR (KBr),  $\nu$  (cm<sup>-1</sup>): 2158 (s, C≡C), 1733 (s, C=O). <sup>1</sup>H NMR (300 MHz, CDCl<sub>3</sub>),  $\delta$  (TMS, ppm): 7.4 (m, 2H, aromatic protons *m* to -O-), 6.8 (m, 2H, aromatic protons *o* to -O-), 3.9 (m, 2H, PhOCH<sub>2</sub>), 3.7 (s, 3H, OCH<sub>3</sub>), 2.3 (m, 2H, CH<sub>2</sub>CO<sub>2</sub>-

CH<sub>3</sub>), 1.8 (m, 2H, PhOCH<sub>2</sub>CH<sub>2</sub>), 1.6 (m, 2H, CH<sub>2</sub>CH<sub>2</sub>CO<sub>2</sub>CH<sub>3</sub>), 1.5–1.3 (m, 12H, (CH<sub>2</sub>)<sub>6</sub>), 0.2 (s, 9H, (CH<sub>3</sub>)<sub>3</sub>Si).

**11-(4-Ethynylphenoxy)undecanoic Acid (13).** Into a 100 mL round-bottom flask equipped with a reflux condenser were placed 2.10 g (5.4 mmol) of **12** and 50 mL of a 4% (w/v) methanol solution of potassium hydroxide. The mixture was refluxed for 4 h and was then poured into 100 mL of 1 M hydrochloric acid. The isolated product was obtained by filtration and dried in a vacuum oven at room temperature (pale yellow solid; yield: 95.1%). IR (KBr),  $\nu$  (cm<sup>-1</sup>): 3285 (s, ≡C–H), 2105 (m, C≡C), 1700 (s, C=O). <sup>1</sup>H NMR (300 MHz, CDCl<sub>3</sub>),  $\delta$  (TMS, ppm): 7.4 (m, 2H, aromatic protons *m* to –O–), 6.8 (m, 2H, aromatic protons *o* to –O–), 3.9 (m, 2H, PhOCH<sub>2</sub>), 3.0 (s, 1H, ≡CH), 2.3 (m, 2H, CH<sub>2</sub>CO<sub>2</sub>H), 1.8 (m, 2H, PhOCH<sub>2</sub>CH<sub>2</sub>), 1.6 (m, 2H, CH<sub>2</sub>CH<sub>2</sub>CO<sub>2</sub>H), 1.5–1.3 (m, 12H, (CH<sub>2</sub>)<sub>6</sub>).

**11-(4-Ethynylphenoxy)undecanoyl-L-leucine Methyl Ester (14).** In a 250 mL round-bottom flask, 2.0 g (6.6 mmol) of **13**, 1.25 g (6.9 mmol) of **5**, and 36 mg (0.27 mmol) of DMAP were dissolved in 100 mL of dry DCM. The solution was cooled with an ice–water bath, to which a DCM (50 mL) solution of DCC (1.65 g, 8.0 mmol) was added slowly with stirring through a dropping funnel with a pressure-equalization arm. The reaction mixture was stirred overnight. After filtration of the solids, the filtrate was concentrated by a rotary evaporator. The crude product was purified on a silica gel column using CHCl<sub>3</sub>/acetone (20/1 by volume) mixture as eluent. Removal of the solvents yielded 1.85 g of white solid of **14** (yield: 65.2%). IR (KBr),  $\nu$  (cm<sup>-1</sup>): 2107 (m, C≡C), 1741 (s, C=O), 1641 (s, C=O). <sup>1</sup>H NMR (300 MHz, CDCl<sub>3</sub>),  $\delta$  (TMS, ppm): 7.4 (m, 2H, aromatic protons *m* to –O–), 6.8 (m, 2H, aromatic protons *o* to –O–), 5.8 (d, 1H, NH), 4.7 (m, 1H, NHCH), 3.9 (m, 2H, PhOCH<sub>2</sub>), 3.7 (s, 3H, CO<sub>2</sub>CH<sub>3</sub>), 3.0 (s, 1H, ≡CH), 2.2 (m, 2H, CH<sub>2</sub>CO<sub>2</sub>NH), 1.8–1.6 (m, 7H, PhOCH<sub>2</sub>CH<sub>2</sub>, NHCHCHCH<sub>2</sub>, CH<sub>2</sub>CH<sub>2</sub>CO<sub>2</sub>NH), 1.5–1.3 (m, 12H, (CH<sub>2</sub>)<sub>6</sub>), 1.0 (m, 6H, (CH<sub>3</sub>)<sub>2</sub>). <sup>13</sup>C NMR (75 MHz, CDCl<sub>3</sub>),  $\delta$  (CDCl<sub>3</sub>, ppm): 173.6 (CO<sub>2</sub>), 172.7 (CONH), 159.4 (aromatic carbon attached to –O–), 133.4 (aromatic carbons *m* to –O–), 114.3 (aromatic carbons *o* to –O–), 113.7 (aromatic carbon *p* to –O–), 83.0 (PhC≡), 75.5 (HC≡), 67.9 (PhOCH<sub>2</sub>), 52.1 (CO<sub>2</sub>CH<sub>3</sub>), 50.4 (NHCH), 41.6 (NHCHCH<sub>2</sub>), 36.4 (CH<sub>2</sub>CO<sub>2</sub>NH), 29.3–29.0 (CH<sub>2</sub>), 25.8 (PhOCH<sub>2</sub>CH<sub>2</sub>), 24.7 (CH, CH<sub>2</sub>CH<sub>2</sub>CO<sub>2</sub>NH), 22.7, 21.8 ((CH<sub>3</sub>)<sub>2</sub>). [ $\alpha$ ]<sub>D</sub><sup>20</sup> +1.6° (c 1.644, chloroform).

**Polymerization.** All the polymerization reactions and manipulations were carried out under nitrogen using Schlenk techniques in a vacuum-line systems except for the purification of the resultant polymers, which was done in a fume hood. A typical experimental procedure for the polymerization of **6** is given below.

**Poly(4-ethynylbenzoyl-L-leucine methyl ester) (1e).** Into a 20 mL Schlenk tube with a sidearm was added 0.2 mmol of **6**. The tube was evacuated under vacuum and then flushed with dry nitrogen three times through the sidearm. THF (1 mL) was injected into the tube to dissolve the monomer. The catalyst solution was prepared in another tube by dissolving [Rh(nbd)Cl]<sub>2</sub> (0.01 mmol) in 1 mL of THF with 1 drop of TEA, which was transferred to the monomer solution using a hypodermic syringe. The reaction mixture was stirred at room temperature under nitrogen for 24 h. The mixture was then diluted with 2 mL of THF and added dropwise to an acetone/diethyl ether mixture (150 mL) under stirring. The precipitate was collected by filtration and dried under vacuum at room temperature to a constant weight. The polymeric product was isolated as yellowish fibrous solid in a high yield (91.7%). *M*<sub>w</sub>: 416 000 (a polymer with an *M*<sub>w</sub> of 1470 000 was obtained when [cat.] was decreased from 5 to 1 mM), *M*<sub>w</sub>/*M*<sub>n</sub>: 3.54 (GPC, polystyrene calibration). IR (KBr),  $\nu$  (cm<sup>-1</sup>): 3031 (w, =CH), 1742 (s, C=O), 1648 (s, C=O). <sup>1</sup>H NMR (400 MHz, acetone-*d*<sub>6</sub>),  $\delta$  (TMS, ppm): 8.0 (NH), 7.6 (aromatic protons *o* to C=O), 6.7 (aromatic protons *m* to C=O), 5.9 (*Z* olefin proton), 4.7 (NHCH), 3.6 (CO<sub>2</sub>CH<sub>3</sub>), 1.7 (CH<sub>2</sub>CH), 0.9 ((CH<sub>3</sub>)<sub>2</sub>). <sup>13</sup>C NMR (100 MHz, acetone-*d*<sub>6</sub>),  $\delta$  (TMS, ppm): 173.8 (CO<sub>2</sub>), 167.5 (CONH), 145.8 (=C–), 139.5 (aromatic carbon *p* to C=O), 134.0 (aromatic carbon attached to C=O), 128.1 (H–C=, aromatic carbons *o* and *m* to C=O), 52.3 (CO<sub>2</sub>CH<sub>3</sub>, NHCH), 41.0 (CH<sub>2</sub>),

25.7 (CH), 23.2, 22.0 ((CH<sub>3</sub>)<sub>2</sub>). UV (MeOH, 1.76 × 10<sup>-4</sup> mol/L),  $\lambda$ <sub>max</sub> (nm)/ $\epsilon$ <sub>max</sub> (mol<sup>-1</sup> L cm<sup>-1</sup>): 274/9.60 × 10<sup>3</sup>, 399/3.65 × 10<sup>3</sup>. [ $\alpha$ ]<sub>D</sub><sup>20</sup> –737.7° (c 0.132, chloroform).

**Poly[11-(4-ethynylphenoxy)undecanoyl-L-leucine methyl ester] (2e).** It was synthesized by a reaction procedure similar to that described above except using **14** as monomer. Brownish yellow solid product; yield: 99.0%. *M*<sub>w</sub>: 20 000, *M*<sub>w</sub>/*M*<sub>n</sub>: 2.84 (GPC, polystyrene calibration). IR (KBr),  $\nu$  (cm<sup>-1</sup>): 3066 (w, =CH), 1748 (s, C=O), 1648 (s, C=O). <sup>1</sup>H NMR (300 MHz, CDCl<sub>3</sub>),  $\delta$  (TMS, ppm): 6.6 (aromatic protons *m* to –O–), 6.4 (aromatic protons *o* to –O–), 5.7 (*Z* olefin proton), 4.6 (NHCH), 3.9 (PhOCH<sub>2</sub>), 3.7 (CO<sub>2</sub>CH<sub>3</sub>), 2.2 (CH<sub>2</sub>CO<sub>2</sub>NH), 1.8–1.3 (PhOCH<sub>2</sub>CH<sub>2</sub>, CH<sub>2</sub>CH<sub>2</sub>CO<sub>2</sub>CH<sub>2</sub>, NHCHCHCH<sub>2</sub>, CH<sub>2</sub>), 0.9 ((CH<sub>3</sub>)<sub>2</sub>). UV (CHCl<sub>3</sub>, 1.33 × 10<sup>-4</sup> mol/L),  $\lambda$ <sub>max</sub> (nm)/ $\epsilon$ <sub>max</sub> (mol<sup>-1</sup> L cm<sup>-1</sup>): 270/7.06 × 10<sup>3</sup>, 395/1.90 × 10<sup>3</sup>. [ $\alpha$ ]<sub>D</sub><sup>20</sup> ~0° (c 0.5, chloroform).

**Hydrolysis.** The ester groups of polyesters **1e** and **2e** were selectively hydrolyzed under a basic condition. A typical experimental procedure for the hydrolysis of **1e** to polyacid **1a** is given below.

**Poly(4-ethynylbenzoyl-L-leucine) (1a).** To a 50 mL round-bottom flask were added 211 mg (0.77 mmol) of **1e** and a methanolic solution of potassium hydroxide (2 g of potassium hydroxide in 20 mL of methanol). After 2 h stirring at room temperature, the mixture was poured into a dilute aqueous hydrochloric acid solution. The precipitate was collected by filtration and dried under vacuum to a constant weight. The polyacid **1a** was isolated as yellowish solid in 95.2% yield. *M*<sub>w</sub>: 1050 000, *M*<sub>w</sub>/*M*<sub>n</sub>: 13.8 (GPC, polystyrene calibration). IR (KBr),  $\nu$  (cm<sup>-1</sup>): 3032 (w, =CH), 1721 (s, C=O), 1643 (s, C=O). <sup>1</sup>H NMR (300 MHz, DMSO-*d*<sub>6</sub>),  $\delta$  (DMSO-*d*<sub>6</sub>, ppm): 12.6 (CO<sub>2</sub>H), 8.4 (NH), 7.7 (aromatic protons *o* to C=O), 6.8 (aromatic protons *m* to C=O), 5.8 (*Z* olefin proton), 4.5 (NHCH), 1.7 (CH<sub>2</sub>CH), 0.9 ((CH<sub>3</sub>)<sub>2</sub>). <sup>13</sup>C NMR (100 MHz, CD<sub>3</sub>OD),  $\delta$  (TMS, ppm): 176.0 (CO<sub>2</sub>), 169.2 (CONH), 146.8 (=C–), 140.3 (aromatic carbon *p* to C=O), 133.7 (aromatic carbon attached to C=O), 128.5 (H–C=, aromatic carbons *o* and *m* to C=O), 52.7 (NHCH), 41.2 (CH<sub>2</sub>), 26.2 (CH), 23.4, 22.0 ((CH<sub>3</sub>)<sub>2</sub>). UV (MeOH, 1.31 × 10<sup>-4</sup> mol/L),  $\lambda$ <sub>max</sub> (nm)/ $\epsilon$ <sub>max</sub> (mol<sup>-1</sup> L cm<sup>-1</sup>): 272/8.92 × 10<sup>3</sup>, 395/3.25 × 10<sup>3</sup>. [ $\alpha$ ]<sub>D</sub><sup>20</sup> –606.7° [c 0.045, methanol/chloroform (3:7 v/v)].

**Poly[11-(4-ethynylphenoxy)undecanoyl-L-leucine] (2a).** The hydrolysis of **2e** was conducted in a similar way as described above. Brownish yellow solid product; yield: 97.5%. *M*<sub>w</sub>: 15 300, *M*<sub>w</sub>/*M*<sub>n</sub>: 1.5 (GPC, polystyrene calibration). IR (KBr),  $\nu$  (cm<sup>-1</sup>): 3061 (w, =CH), 1749 (s, C=O), 1648 (s, C=O). <sup>1</sup>H NMR (300 MHz, CD<sub>3</sub>OD),  $\delta$  (CD<sub>3</sub>OD, ppm): 6.6 (aromatic protons *m* to –O–), 6.4 (aromatic protons *o* to –O–), 5.8 (*Z* olefin proton), 4.4 (NHCH), 4.2 (CO<sub>2</sub>CH<sub>2</sub>), 3.9 (PhOCH<sub>2</sub>), 2.2 (CH<sub>2</sub>CO<sub>2</sub>CH<sub>2</sub>), 1.8–1.5 (PhOCH<sub>2</sub>CH<sub>2</sub>, NHCHCHCH<sub>2</sub>, CH<sub>2</sub>CH<sub>2</sub>CO<sub>2</sub>CH<sub>2</sub>), 1.5–1.1 ((CH<sub>2</sub>)<sub>6</sub>), 0.9 ((CH<sub>3</sub>)<sub>2</sub>). UV (MeOH, 1.19 × 10<sup>-4</sup> mol/L),  $\lambda$ <sub>max</sub> (nm)/ $\epsilon$ <sub>max</sub> (mol<sup>-1</sup> L cm<sup>-1</sup>): 265/8.05 × 10<sup>3</sup>, 395/2.24 × 10<sup>3</sup>. [ $\alpha$ ]<sub>D</sub><sup>20</sup> ~0° [c 0.3, NaOH/H<sub>2</sub>O (0.2 M)].

**Acknowledgment.** The work described in this paper was partially supported by the Research Grants Council of Hong Kong (Projects HKUST 6187/99P, 6121/01P, and 6085/02P). This project also benefited from the financial support of the University Grants Committee of Hong Kong through an Area of Excellence Scheme (Grant AoE/P-10/01-1-A).

**Supporting Information Available:** Figure showing the <sup>1</sup>H NMR spectrum of **1e** in methanol-*d*<sub>4</sub>. This material is available free of charge via the Internet at <http://pubs.acs.org>.

## References and Notes

- (1) (a) Johnson, G. B. *The Living World*, 2nd ed.; McGraw-Hill: Boston, 2000. (b) Zubay, G. L. *Biochemistry*, 4th ed.; Wm. C. Brown Publishers: Boston, 1998.
- (2) (a) *The Amphipathic Helix*; Epanand, R. M., Ed.; CRC: Boca Raton, FL, 1993. (b) *Patterns in Protein Sequence and Structure*; Taylor, W. R., Ed.; Springer-Verlag: Hong Kong, 1992.

- (3) (a) Jeffrey, G. A. *An Introduction to Hydrogen Bonding*; Oxford University Press: New York, 1997. (b) Jeffrey, G. A.; Saenger, W. *Hydrogen Bonding in Biological Structures*; Springer-Verlag: Hong Kong, 1994.
- (4) For selected examples of reviews on helical polymers, see: (a) Ciferri, A. *Macromol. Rapid Commun.* **2002**, *23*, 511–529. (b) James, T. D.; Shinkai, S. *Top. Curr. Chem.* **2002**, *218*, 159–200. (c) Cornelissen, J. J. L. M.; Rowan, A. E.; Nolte, R. J. M.; Sommerdijk, N. A. J. M. *Chem. Rev.* **2001**, *101*, 4039–4070. (d) Nakano, T.; Okamoto, Y. *Chem. Rev.* **2001**, *101*, 4013–4038. (e) Green, M. M.; Cheon, K. S.; Yang, S. Y.; Park, J. W.; Swansburg, S.; Liu, W. H. *Acc. Chem. Res.* **2001**, *34*, 672–680. (f) Fujiki, M. *Macromol. Rapid Commun.* **2001**, *22*, 539–563. (g) Pu, L. *Chem. Rev.* **1998**, *98*, 2405–2494. (h) Moore, J. S. *Curr. Opin. Solid State Mater. Sci.* **1996**, *1*, 777–787. (i) Lawrence, D. S.; Jiang, T.; Levett, M. *Chem. Rev.* **1995**, *95*, 2229–2260.
- (5) (a) Bushey, M. L.; Hwang, A.; Stephens, P. W.; Nuckolls, C. *Angew. Chem., Int. Ed.* **2002**, *41*, 2828–2833. (b) Yamauchi, K.; Lizotte, J. R.; Hercules, D. M.; Vergne, M. J.; Long, T. E. *J. Am. Chem. Soc.* **2002**, *124*, 8599–8604. (c) Duffy, D. M.; Rodger, P. M. *J. Am. Chem. Soc.* **2002**, *124*, 5206–5212. (d) Brunsveld, L.; Vekemans, J. A. J. M.; Hirschberg, J. H. K. K.; Sijbesma, R. P.; Meijer, E. W. *Proc. Natl. Acad. Sci. U.S.A.* **2002**, *99*, 4977–4982. (e) Kennedy, R. J.; Tsang, K. Y.; Kemp, D. S. *J. Am. Chem. Soc.* **2002**, *124*, 934–944. (f) Cornelissen, J. J. L. M.; Donners, J. J. J. M.; de Gelder, R.; Graswinckel, W. S.; Metselaar, G. A.; Rowan, A. E.; Sommerdijk, N. A. J. M.; Nolte, R. J. M. *Science* **2001**, *293*, 676–680. (g) Klok, H. A.; Langenwalter, J. F.; Lecommandoux, S. *Macromolecules* **2000**, *33*, 7819–7826. (h) Berl, V.; Huc, I.; Khoury, R. G.; Krische, M. J.; Lehn, J. M. *Nature (London)* **2000**, *407*, 720–723. (i) Hirschberg, J. H. K. K.; Brunsveld, L.; Ramzi, A.; Vekemans, J. A. J. M.; Sijbesma, R. P.; Meijer, E. W. *Nature (London)* **2000**, *407*, 167–170. (j) Cheng, Q.; Yamamoto, M.; Stevens, R. C. *Langmuir* **2000**, *16*, 5333–5342.
- (6) (a) Srinivasan, R.; Rose, G. D. *Proc. Natl. Acad. Sci. U.S.A.* **1999**, *96*, 14258–14263. (b) Appella, D. H.; Christianson, L. A.; Klein, D. A.; Richards, M. R.; Powell, D. R.; Gellman, S. H. *J. Am. Chem. Soc.* **1999**, *121*, 7574–7581. (c) Prins, L. J.; Huskens, J.; de Jong, F.; Timmerman, P.; Reinhoudt, D. N. *Nature (London)* **1999**, *398*, 498–502. (d) Amabilino, D. B.; Ramos, E.; Serrano, J. L.; Sierra, T.; Veciana, J. *J. Am. Chem. Soc.* **1998**, *120*, 9126–9134. (e) Kurihara, S.; Mori, T.; Nonaka, T. *Macromolecules* **1998**, *31*, 5940–5942. (f) Amabilino, D. B.; Ramos, E.; Serrano, J. L.; Sierra, T.; Veciana, J. *J. Am. Chem. Soc.* **1998**, *120*, 9126–9134. (g) Appella, D. H.; Christianson, L. A.; Klein, D. A.; Powell, D. R.; Huang, X. L.; Barchi, J. J.; Gellman, S. H. *Nature (London)* **1997**, *387*, 381–384.
- (7) (a) Nishimura, T.; Takatani, K.; Sakurai, S.; Maeda, K.; Yashima, E. *Angew. Chem., Int. Ed.* **2002**, *41*, 3602–3604. (b) Tabei, J.; Nomura, R.; Masuda, T. *Macromolecules* **2002**, *35*, 5405–5409. (c) Nomura, R.; Tabei, J.; Masuda, T. *J. Am. Chem. Soc.* **2001**, *123*, 8430–8431. (d) Saito, M. A.; Maeda, K.; Onouchi, H.; Yashima, E. *Macromolecules* **2000**, *33*, 4616–4618. (e) Yashima, E.; Maeda, K.; Okamoto, Y. *Nature (London)* **1999**, *399*, 449–451. (f) Akagi, K.; Piao, G.; Kaneko, S.; Sakamaki, K.; Shirakawa, H.; Kyotani, M. *Science* **1998**, *282*, 1683–1686.
- (8) For reviews, see: (a) Cheuk, K. K. L.; Li, B. S.; Tang, B. Z. *Curr. Trends Polym. Sci.* **2002**, *7*, 41–55. (b) Tang, B. Z. *Polym. News* **2001**, *26*, 262–272. (c) Tang, B. Z.; Cheuk, K. K. L.; Salhi, F.; Li, B.; Lam, J. W. Y.; Cha, J. A. K.; Xiao, X. *ACS Symp. Ser.* **2001**, *812*, 133–148. (d) Cheuk, K. K. L.; Li, B. S.; Tang, B. Z. In *Encyclopedia of Nanoscience and Nanotechnology*; Nalwa, H. S., Ed.; American Scientific Publishers: Stevenson Ranch, CA, in press.
- (9) (a) Cheuk, K. K. L.; Lam, J. W. Y.; Sun, Q.; Cha, J. A. K.; Tang, B. Z. *Polym. Prepr.* **1999**, *40* (2), 653–654. (b) Cheuk, K. K. L.; Lam, J. W. Y.; Sun, Q.; Cha, J. A. K.; Tang, B. Z. *Polym. Prepr.* **1999**, *40* (2), 655–656. (c) Cheuk, K. K. L. Ph.D. Dissertation, Hong Kong University of Science & Technology, Feb 2002.
- (10) (a) Nicolini, C. A. *Molecular Bioelectronics*; World Scientific: Hong Kong, 1996. (b) Yalpani, M. *Biomedical Functions and Biotechnology of Natural and Artificial Polymers*; ATL Press: Mount Prospect, IL, 1996. (c) *Biomedical Materials-Drug Delivery, Implants, and Tissue Engineering*; Neenan, T.; Marcolongo, M.; Valentini, R. F., Eds.; MRS: Warrendale, PA, 1999. (d) Nolfi, S.; Floreano, D. *Evolutionary Robotics: the Biology, Intelligence, and Technology of Self-organizing Machines*; MIT Press: Cambridge, MA, 2000.
- (11) (a) Li, B.; Cheuk, K. K. L.; Ling, L.; Chen, J.; Xiao, X.; Bai, C.; Tang, B. Z. *Macromolecules* **2003**, *36*, 77–85. (b) Li, B.; Cheuk, K. K. L.; Salhi, F.; Lam, J. W. Y.; Cha, J. A. K.; Xiao, X.; Bai, C.; Tang, B. Z. *Nano Lett.* **2001**, *1*, 323–328. (c) Salhi, F.; Cheuk, K. K. L.; Sun, Q.; Lam, J. W. Y.; Cha, J. A. K.; Li, G.; Li, B.; Luo, J.; Chen, J.; Tang, B. Z. *J. Nanosci. Nanotechnol.* **2001**, *1*, 137–141.
- (12) (a) Mylnikov, V. S. *Adv. Polym. Sci.* **1994**, *115*, 1–88. (b) Mi, Y.; Tang, B. Z. *Polym. News* **2001**, *26*, 170–176. (c) Kang, E. T.; Ehrlich, P.; Bhatt, A. P.; Anderson, W. A. *Macromolecules* **1984**, *17*, 1020–1024. (b) Zhao, J.; Yang, M.; Shen, Z. *Polym. J.* **1991**, *23*, 963–968. (c) Vohlidal, J.; Sedlacek, J.; Pacovska, M.; Lavastre, O.; Dixneuf, P. H.; Balcar, H.; Pflayer, J. *Polymer* **1997**, *38*, 3359–3367. (d) Tang, B. Z.; Chen, H. Z.; Xu, R. S.; Lam, J. W. Y.; Cheuk, K. K. L.; Wong, H. N. C.; Wang, M. *Chem. Mater.* **2000**, *12*, 213–221. (e) Sun, J. Z.; Chen, H. Z.; Xu, R. S.; Wang, M.; Lam, J. W. Y.; Tang, B. Z. *Chem. Commun.* **2002**, 1222–1223.
- (13) (a) Tang, B. Z.; Kong, X.; Wan, X.; Feng, X.-D. *Macromolecules* **1997**, *30*, 5620–5628. (b) Tang, B. Z.; Kong, X.; Wan, X.; Feng, X.-D. *Macromolecules* **1998**, *31*, 7118.
- (14) (a) Branden, C.; Tooze, J. *Introduction to Protein Structure*, 2nd ed.; Garland Pub.: New York, 1999. (c) *Amino Acids, Peptides, and Proteins*; Royal Society of Chemistry: Cambridge, 1994.
- (15) (a) Syud, F. A.; Stanger, H. E.; Gellman, S. H. *J. Am. Chem. Soc.* **2001**, *123*, 8667–8677. (b) Schmidt, K. S.; Sigel, R. K. O.; Filippov, D. V.; van der Marel, G. A.; Lippert, B.; Reedijk, J. *New J. Chem.* **2000**, *24*, 195–197. (c) Gemmecker, G. *Angew. Chem., Int. Ed.* **2000**, *39*, 1224–1226. (d) Xu, X.-P.; Au-Yeung, S. C. F. *J. Phys. Chem. B* **2000**, *104*, 5641–5650. (e) Barchi, J. J.; Huang, X. L.; Appella, D. H.; Christianson, L. A.; Durell, S. R.; Gellman, S. H. *J. Am. Chem. Soc.* **2000**, *122*, 2711–2718. (f) Zeng, H. Q.; Miller, R. S.; Flowers, R. A.; Gong, B. *J. Am. Chem. Soc.* **2000**, *122*, 2635–2644. (g) Yashima, E.; Matsushima, T.; Okamoto, Y. *J. Am. Chem. Soc.* **1997**, *119*, 6345–6359.
- (16) (a) Pretsch, E.; Bühlmann, P.; Affolter, C. *Structure Determination of Organic Compounds: Tables of Spectral Data*, 3rd ed.; Springer: Berlin, 2000. (b) Silverstein, R. M.; Webster, F. X. *Spectrometric Identification of Organic Compounds*, 6th ed.; Wiley: New York, 1998. (c) Lambert, J. B.; Shurvell, H. F.; Lightner, D. A.; Cooks, R. G. *Organic Structural Spectroscopy*; Prentice Hall: Englewood Cliffs, NJ, 1998.
- (17) For selected reviews, see: (a) Masuda, T.; Higashimura, T. *Adv. Polym. Sci.* **1987**, *81*, 121. (b) Ginsburg, E. J.; Gorman, C. B.; Grubbs, R. H. In *Modern Acetylene Chemistry*; Stang, P. J., Diederich, F., Eds.; VCH: New York, 1995; Chapter 10, pp 353–383. (c) Tabata, M.; Stone, T.; Sadahiro, Y. *Macromol. Chem. Phys.* **1999**, *200*, 265–282. (d) Choi, S. K.; Gal, Y. S.; Jin, S. H.; Kim, H. K. *Chem. Rev.* **2000**, *100*, 1645–1681.
- (18) (a) Yao, G.; Dong, Y.; Cao, T.; Yang, S.; Lam, J. W. Y.; Tang, B. Z. *J. Colloid Interface Sci.* **2003**, *257*, 263–267. (b) Tang, B. Z.; Xu, H. *Macromolecules* **1999**, *32*, 2569–2576. (c) Kong, X.; Lam, J. W. Y.; Tang, B. Z. *Macromolecules* **1999**, *32*, 1722–1730.
- (19) Cheuk, K. K. L.; Luo, J.; Lam, J. W. Y.; Tang, B. Z. *Polym. Prepr.* **2001**, *42* (1), 545–546.
- (20) Chen, J.; Lam, J. W. Y.; Cheuk, K. K. L.; Xie, Z.; Peng, H.; Lai, L. M.; Tang, B. Z. *Polym. Mater. Sci. Eng.* **2002**, *86*, 179–180.
- (21) Carey, F. A.; Sundberg, R. J. *Advanced Organic Chemistry*, 4th ed.; Plenum: New York, 2001.
- (22) (a) Robertson, J. *Protecting Group Chemistry*; Oxford University Press: New York, 2000. (b) Kocienski, P. J. *Protecting Groups*; G. Thieme: New York, 2000. (c) Greene, T. W.; Wuts, P. G. M. *Protective Groups in Organic Synthesis*, 3rd ed.; Wiley: New York, 1999.
- (23) (a) Kong, X.; Lam, J. W. Y.; Tang, B. Z. *Macromolecules* **1999**, *32*, 1722–1730. (b) Lam, J. W. Y.; Kong, X.; Dong, Y.; Cheuk, K. K. L.; Xu, K.; Tang, B. Z. *Macromolecules* **2000**, *33*, 5027–5040. (c) Lam, J. W. Y.; Dong, Y.; Cheuk, K. K. L.; Luo, J.; Xie, Z.; Kwok, H. S.; Mo, Z.; Tang, B. Z. *Macromolecules* **2002**, *35*, 1229–1240. (d) Lam, J. W. Y.; Tang, B. Z. *J. Polym. Sci., Part A: Polym. Chem.* **2003**, *41*, in press. (e) Lam, J. W. Y.; Cheuk, K. K. L.; Tang, B. Z. *Polym. Mater. Sci. Eng.* **2003**, *88*, in press.
- (24) (a) Simionescu, C. I.; Percec, V.; Dumitrescu, S. *J. Polym. Sci., Polym. Chem. Ed.* **1977**, *15*, 2497–2509. (b) Simionescu, C. I.; Percec, V. *J. Polym. Sci., Polym. Symp.* **1980**, *67*, 43–71. (c) Percec, V.; Obata, M.; Rudick, J. G.; De, B. B.; Glodde,

- M.; Bera, T. K.; Magonov, S. N.; Balagurusamy, V. S. K.; Heiney, P. A. *J. Polym. Sci., Part A: Polym. Chem.* **2002**, *40*, 3509–3533. (d) Percec, V.; Rudick, J. G.; Nombel, P.; Buchowicz, W. *J. Polym. Sci., Part A: Polym. Chem.* **2002**, *40*, 3212–3220.
- (25) Ito, T.; Shirakawa, H.; Ikeda, S. *J. Polym. Sci., Polym. Chem. Ed.* **1975**, *13*, 1934–1938.
- (26) (a) Masuda, T.; Tang, B. Z.; Tanaka, T.; Higashimura, T. *Macromolecules* **1986**, *19*, 1459–1464. (b) Seki, H.; Tang, B. Z.; Tanaka, A.; Masuda, T. *Polymer* **1994**, *35*, 3456–3462.
- (27) Indeed, the polymer chains readily self-associate: when a polymer solution is precipitated into a poor solvent, the solubility of the polymer decreases. Repeating the precipitation process several times results in the formation of partially insoluble aggregates due to self-assembling of the amphiphilic chains through hydrogen-bond formation.
- (28) (a) *CRC Handbook of Chemistry and Physics*, 75th ed.; Lide, D. R., Ed.; CRC Press: Boca Raton, FL, 1994; pp 6-155–6-188. (b) Debye, P. *Polar Molecules*; Dover: New York, 1945.
- (29) (a) *Circular Dichroism: Principles and Applications*; Berova, N., Nakanishi, K., Woody, R. W., Eds.; Wiley-VCH: New York, 2000. (b) Lightner, D. A.; Gurst, J. E. *Organic Conformational Analysis and Stereochemistry from Circular Dichroism Spectroscopy*; Wiley-VCH: New York, 2000.
- (30) (a) Nakashima, H.; Fujiki, M.; Koe, J. R.; Motonaga, M. *J. Am. Chem. Soc.* **2001**, *123*, 1963–1969. (b) Brunsveld, L.; Meijer, E. W.; Prince, R. B.; Moore, J. S. *J. Am. Chem. Soc.* **2001**, *123*, 7978–7984. (c) Jung, J. H.; Kobayashi, H.; Masuda, M.; Shimizu, T.; Shinkai, S. *J. Am. Chem. Soc.* **2001**, *123*, 8785–8789. (d) Huang, X.; Liu, M. *Chem. Commun.* **2003**, 66–67. (e) Tang, B. Z. *Heart Cut Feb* 10, 2003.
- (31) (a) Hawker, C. J. *Adv. Polym. Sci.* **1999**, *147*, 113–160. (b) Cornelissen, J. J. L. M.; Peeters, E.; Janssen, R. A. J.; Meijer, E. W. *Acta Polym.* **1998**, *49*, 471–476. (c) Devadoss, C.; Bharathi, P.; Moore, J. S. *Angew. Chem., Int. Ed.* **1997**, *36*, 1633–1635. (d) Chen, J.; Xie, Z.; Lam, J. W. Y.; Law, C. C. W.; Tang, B. Z. *Macromolecules* **2003**, *36*, 1108–1117. (e) Tang, B. Z.; Poon, W. H.; Peng, H.; Wong, H. N. C.; Ye, X.; Monde, T. *Chin. J. Polym. Sci.* **1999**, *17*, 81–86.
- (32) Tabei, J.; Nomura, R.; Masuda, T. *Macromolecules* **2003**, *36*, 573–577.
- (33) Gu, H.; Nakamura, Y.; Sato, T.; Teramoto, A.; Green, M. M.; Jha, S. K.; Andreola, C.; Reidy, M. P. *Macromolecules* **1998**, *31*, 6362–6368. (b) Fiesel, R.; Scherf, U. *Acta Polym.* **1998**, *49*, 445–449.
- (34) (a) Cheuk, K. K. L.; Li, B. S.; Salhi, F.; Lam, J. W. Y.; Cha, J. A. K.; Tang, B. Z. *Polym. Mater. Sci. Eng.* **2001**, *84*, 536–537. (b) Li, B.; Cheuk, K. K. L.; Yang, D.; Lam, J. W. Y.; Wan, L.; Bai, C.; Tang, B. Z. *Macromolecules* **2003**, *36*, in press.
- (35) (a) Li, B. S.; Cheuk, K. K. L.; Zhou, J.; Xie, Y.; Tang, B. Z. *Polym. Mater. Sci. Eng.* **2001**, *85*, 401–402. (b) Cheuk, K. K. L.; Li, B. S.; Chen, J. W.; Xie, Y.; Tang, B. Z. *Proc. 5th Asian Symp. Biomed. Mater.* **2001**, 514–518.
- (36) Tang, B. Z.; Poon, W. H.; Leung, S. M.; Leung, W. H.; Peng, H. *Macromolecules* **1997**, *30*, 2209–2212.

MA0344543